R. & M. No. 2596
(11,542)
A.R.C. Technical Report

MINISTRY OF SUPPLY

AERONAUTICAL RESEARCH COUNCIL
REPORTS AND MEMORANDA

Calculated Loadings due to Incidence of a Number of Straight and Swept-back Wings

By

V. M. FALKNER, B.Sc., A.M.I.Mech.E., with Appendix by
DORIS LEHRIAN, B.Sc., of the Aerodynamics Division, N.P.L.

LONDON: HER MAJESTY'S STATIONERY OFFICE
1952
TWELVE SHILLINGS NET

Calculated Loadings due to Incidence of a Number of Straight and Swept-back Wings

By

V. M. Falkner, B.Sc., A.M.I.Mech.E.

with Appendix by Doris Lehrian, B.Sc.
of the Aerodynamics Division, N.P.L.

Reports and Memoranda No. 2596

June, 1948

Summary.—In this report are collected together the calculated aerodynamic loadings due to incidence of a number of straight and swept-back wings. The calculations follow in the main the routine described previously in another report[1], but include additions concerned with induced camber and induced drag. An additional investigation is made of the effect of the N.A.C.A. camber on the properties at zero lift of a rectangular wing of aspect ratio 6.

A table is given of loading functions for use in auxiliary solutions when the wing plan has a discontinuity of direction at an arbitrary position along the span.

1. *Introduction.*—In this report are collected together the calculated aerodynamic loadings due to incidence of a number of straight and swept-back wings. The calculations are based on the vortex-lattice method described in Ref. 1, but have additional interest in that the full effects of the discontinuity at the median section are now apparent, and calculations relating to induced camber and induced drag are included.

A further extension is that the auxiliary loading functions required to allow for the effect of the discontinuity in plan, when this occurs at the median section, have been established as dependent on the aspect ratio only.

2. *Range of Solutions.*—The wings described in this report include twelve wings of constant chord, of aspect ratios 6, 4, 2 and 1 and with angles of sweep-back 0, 30 and 45 deg, a triangular wing with 90 deg apex angle, aspect ratio 4; and two other wings derived from the latter by cropping the tips to reduce to aspect ratios 3 and 2·309 respectively. Results for other wings will be included in a later report.

The work includes calculation of the lift, local lift coefficient (C_{LL}/C_L), loading coefficient $(C_{LL}c/C_L\bar{c})$, local aerodynamic centre, induced drag and in some cases the induced camber.

Some wind-tunnel results which show the overall agreement between theoretical and experimental results are included.

3. *Loading Functions.*—All of the wings dealt with in this report have the discontinuity of leading edge at the wing centre, and it has been shown in Ref. 1 that solutions are obtained by first calculating the standard solution for control points at 0·2, 0·6 and 0·8 and modifying

this by a 'rounding off' solution involving the use of special circulation functions of which the induced downwash curve is polygonal. For cases with the discontinuity at the median section, the special functions for incidence solutions are built up from the two functions P_a and P_b which have double values and which, described previously in Ref. 1, are now given again in Table 1. Various combinations of the functions are given in Table 2, and in every case the $0 \cdot 1$ lattice values are to be used in the lattice for finding the expressions for the downwash at the control points, while the true values are to be used in the analysis subsequent to the establishment of the formula for the vortex sheet. Although such cases are not treated here, the presence of discontinuities along the span requires the use of further functions and their interpolates if necessary, and a range of these, again with double values, is given in Table 3. The distribution of induced downwash for each is symmetrical and of the roof-top type, with apices at different positions along the span, and the values are included in the Tables as well as being plotted for the same cases in Fig. 1.

The functions are derived by combining the Tables of Ref. 2 in certain proportions as follows:—

$$P_a \equiv TF_{00} - 10P_{S00} + 9P_{S10}$$

$$P_b \equiv TF_{00} - 5P_{S00} + 4P_{S20}$$

$$P_1 \equiv 10P_{S00} - 18P_{S10} + 8P_{S20}$$

$$P_2 \equiv 9P_{S10} - 16P_{S20} + 7P_{S30}$$

$$P_3 \equiv 8P_{S20} - 14P_{S30} + 6P_{S40}$$

$$P_4 \equiv 7P_{S30} - 12P_{S40} + 5P_{S50}$$

$$P_5 \equiv 6P_{S40} - 10P_{S50} + 4P_{S60}$$

$$P_6 \equiv 5P_{S50} - 8P_{S60} + 3P_{S70}$$

$$P_7 \equiv 4P_{S60} - 6P_{S70} + 2P_{S80}$$

For each case, the four constants T_{15}, T_{16}, T_{19} and T_{20} are given, where, for $K/4sV = P$ (*see* Ref. 1), $C_L = (8s^2/S)\,T_{15}$, $T_{16} = (16/\pi)\,T_{15}$, the position of the centre-of-pressure of the symmetrical half-wing loading in terms of the semispan is $2T_{19}/T_{15}$, and $P(\eta \to 1) = T_{20}\sqrt{(1 - \eta^2)}$.

3.1. By the use of auxiliary solutions in the region of the discontinuity, which involve control points placed at $\eta = 0$ and $0 \cdot 1$ as well as at the standard positions, the proportions of the two functions P_a and P_b which must be used in the combined function have been estimated for several wings of varying taper, and aspect ratio. The results show that the proportions depend mainly on aspect ratio, and can be selected, without necessity for close accuracy, from the diagram of Fig. 2, which has been plotted from the following data.

A.R.6. Taper 1 to 1: 45 deg sweep.	$0 \cdot 68P_a + 0 \cdot 32P_b$
A.R.4. Taper 1 to 1: 45 deg sweep.	$0 \cdot 66P_a + 0 \cdot 34P_b$
A.R.1. Taper 1 to 1: 45 deg sweep.	$0 \cdot 51P_a + 0 \cdot 49P_b$
Delta wing, equilateral triangle, A.R.2·31.	$0 \cdot 61P_a + 0 \cdot 39P_b$
A.R.5·82. Taper 0·323: 45 deg sweep.	$0 \cdot 66P_a + 0 \cdot 34P_b$

The function for all wings with the discontinuity at the median section can, therefore, be chosen by reference to this diagram, but it must be noted that they will be applicable only to incidence solutions, and that for wing twist different functions are required.

4. *Basis of solutions.*—The solutions are based generally on the following formula for the vortex sheet, as given in A.R.C. Report 10,895:—

$$\frac{kc}{8sV \sin \alpha} = F_0 \cot \tfrac{1}{2}\Theta + F_1 \sin \Theta + F_2 \sin 2\Theta$$

where

$$F_0 = \sqrt{(1-\eta^2)}\,(a_0 + b_0\eta + c_0\eta^2 + \ldots .) + p_0 P$$

$$F_1 = \sqrt{(1-\eta^2)}\,(a_1 + b_1\eta + c_1\eta^2 + \ldots .) + p_1 P$$

$$F_2 = \sqrt{(1-\eta^2)}\,(a_2 + b_2\eta + c_2\eta^2 + \ldots .) + p_2 P$$

where P is the auxiliary function as described in the preceding paragraph. Unless p_0, p_1 and p_2 are zero, the induced drag is not directly calculable, and a numerical integration will be required, based on the general expression for induced drag.

$$C_{DI} = \frac{8s^2}{S} \int_{-1}^{1} \left(\frac{w}{V}\right)\left(\frac{K}{4sV}\right) d\eta \quad .$$

An example of this is given for solution 7 in Table4. The downwash is made up of two parts, the first derived from the Fourier terms, given by

$$\frac{w}{V} = \frac{\Sigma n A_n \sin n\phi}{\sin \phi},$$

and the second from the polygonal distribution associated with the auxiliary functions. The values of sin $n\phi$ are tabulated in Ref. 3.

For

$$\frac{kc}{8sV \sin \alpha} = p_0 P \cot \tfrac{1}{2}\Theta + p_1 P \sin \Theta + p_2 P \sin 2\Theta,$$

$$\frac{K}{4sV \sin \alpha} = \pi\,(p_0 + \tfrac{1}{2}p_1)\,P,$$

and the downwash per radian is $\pi\,(p_0 + \frac{1}{2}p_1)$ at $\eta = 0$, this being the factor to be applied to the standard values for w/V given in Tables 1, 2 and 3.

Instead of the circulation, values will be given of a loading coefficient, defined as $C_{LL}c/C_L\bar{c}$, the advantage being that the area under all curves is unity. For constant chord wings this coefficient is the same as C_{LL}/C_L and the general formula is

$$4\pi A\,(F_0 + \tfrac{1}{2}F_1)/(dc_L/d\alpha) \text{ where } A \text{ is aspect ratio.}$$

5. *Induced Camber.*—The induced camber is defined in the following way—if the downwash due to the chordwise distribution of vorticity be computed on the assumption that the flow is two-dimensional with a straight airstream, the mean camber line would require to be curved in order to satisfy the tangential flow condition. The displacement of this curved camber line from the straight line joining the leading and trailing edges is defined as the induced camber.

5.1. The induced camber is calculated as follows:—

The three-dimensional vorticity distribution on a wing is given by

$$\frac{kc}{8sV \sin \alpha} = F_0 \cot \tfrac{1}{2}\Theta + F_1 \sin \Theta + F_2 \sin 2\Theta .$$

The two-dimensional equivalent is usually written

$$k = 2V\,(A_0 \cot \tfrac{1}{2}\Theta + A_1 \sin \Theta + A_2 \sin 2\Theta)$$

and the two expressions are identical if

$$A_0 = \frac{4s}{c} F_0 \sin \alpha, \quad A_1 = \frac{4s}{c} F_1 \sin \alpha, \text{ etc.}$$

Now the downwash, positive downwards, is given by

$$\frac{w}{V} = A_0 - A_1 \cos \Theta - A_2 \cos 2\Theta .$$

The slope of the camber line is $-w/V$, and the ordinates (z) are obtained by integrating $-w/V$ from the leading edge to the point concerned. Hence,

$$\frac{z}{c} = \frac{1}{c}\int_{c/2}^{x} (A_0 - A_1 \cos \Theta - A_2 \cos 2\Theta)\, dx$$

or since $x = \frac{1}{2}c \cos \Theta$,

$$\frac{z}{c} = -\tfrac{1}{2}\int_{0}^{\Theta} (A_0 - A_1 \cos \Theta - A_2 \cos 2\Theta) \sin \Theta\, d\Theta .$$

Therefore,

$$\frac{z}{c} = \tfrac{1}{2}\Big[A_0 (\cos \Theta - 1) - \tfrac{1}{4}A_1 (\cos 2\Theta - 1) - \tfrac{1}{6}A_2 (\cos 3\Theta - 1) + \tfrac{1}{2}A_2 (\cos \Theta - 1)\Big] .$$

Substituting $\cos \Theta = \xi$,

$$\frac{z}{c} = \tfrac{1}{2}A_0 (\xi - 1) - \tfrac{1}{4}A_1 (\xi^2 - 1) - \tfrac{1}{6}A_2 (2\xi^3 - 3\xi + 1).$$

At the leading edge

$$\xi = 1 \text{ and } z/c = 0,$$

while at the trailing edge,

$$\xi = -1 \text{ and } z/c = -A_0 - \tfrac{1}{3}A_2 .$$

Hence, the induced camber is given by

$$\frac{\textit{camber}}{\textit{chord}} = \tfrac{1}{2}A_0 (\xi - 1) - \tfrac{1}{4}A_1 (\xi^2 - 1) - \tfrac{1}{6}A_2 (2\xi^3 - 3\xi + 1) + (A_0 + \tfrac{1}{3}A_2)\,\frac{1 - \xi}{2}$$

where $(1 - \xi)/2$ is the distance from the leading edge in terms of the chord.

Finally,

$$\frac{\textit{camber}}{\textit{chord}} = \tfrac{1}{4}A_1 (1 - \xi^2) + \tfrac{1}{3}A_2 (\xi - \xi^3) = \frac{s}{c} \sin \alpha\, (1 - \xi^2)\,(F_1 + \tfrac{4}{3}F_2\xi)$$

5.2. From the nature of the calculations by which the coefficients a_0, a_1, etc., are computed, the results for induced camber will not have the same precision as the main properties of the wing. The occurrence of ill-conditioned equations might affect adversely the accuracy of F_1 and F_2, and, when obtained from comparatively few control points, it should be noted that the values of induced camber may sometimes only represent the order of the effect, rather than exact values. Accuracy can, of course, be improved by the use of more control points and normalisation.

6. *Results*.—The results are given in Tables 4 to 40, and, as the calculations follow standard methods, a minimum of explanation will be needed. The induced cambers have all been calculated for $C_L = 1$.

Rectangular wing: aspect ratio 6: 0 *deg sweep-back: Tables* 5 *to* 9.—In this set are included standard solutions with 6 and 9 points using the 84-vortex lattice; a 6-point solution by Blenk[4] revised by Argyris; a lifting-line solution; and a recalculation of α_0 and C_{m0} for the N.A.C.A. camber.

The lifting-plane solutions by the vortex-lattice method are in good general agreement. The solution given by Blenk required revision as it was based on surface integrals which suffered from inaccuracy towards the tips of the wing. The errors have been corrected as the result of an unpublished investigation by Argyris, and the solution now given, which can be taken as based on exact values of downwash integrals at the control points, agrees quite well with the remainder of the calculations, any slight discrepancies being accounted for by the variation in the disposition of the control points. The lifting-line solution has been included in order to show the error involved in this approximation. Solution 5 (*see* R. & M. 1910[5]) was calculated originally by using the actual slopes of the surface at the control points, and is of importance in that it demonstrates the little-known fact that α_0 and C_{m0} are variable with aspect ratio for a uniform cambered wing. The revised calculations, which give α_0 and C_{m0} for aspect ratios 6 and infinity with the position of maximum camber varying from $0 \cdot 2$ to $0 \cdot 7$, are based on equivalent slopes, the origin of which is described in an Appendix to this report.

The complete 9-point equations were used for this work, and, in order to show the effect of varying the number of control points, the case $P = 0 \cdot 2$ has also been calculated for a 6-point solution with two terms chordwise. This gave $\alpha_0 = -1 \cdot 597$ and $C_{m0} = -1 \cdot 744$ instead of $-1 \cdot 633$ and $-1 \cdot 748$ respectively, showing that the important quantity C_{m0} can be calculated quite accurately by the use of six points.

6.1. *Constant-chord wing: aspect ratio* 6: 30 *deg sweep-back: Tables* 10 *and* 11.—The two solutions, standard 6-point and standard 6-point modified, are based on the 126-vortex pattern. The auxiliary loading function used was $0 \cdot 65P_a + 0 \cdot 35P_b$, and the main effect of the modification to 'round off' the discontinuity is to reduce the loading and shift back the local aerodynamic centre at the wing centre, increase the induced drag, and alter appreciably the induced camber. The integration for evaluating the induced drag is given as a typical example in Table 4.

6.2. *Constant-chord wing: aspect ratio* 6: 45 *deg sweep-back: Tables* 12 *to* 18.—For this wing, a comprehensive range of solutions has been calculated. These start with solutions 8, 9 and 10, standard and modified solutions with the 21-vortex pattern, and continue with solution 11, a 126-vortex standard solution, solutions 12 and 14, two auxiliary solutions, and finally solution 13, a full 8-point solution. The first point to be noted is that solution 10, in which P_a and P_b were both used, gives proportions of P_a and P_b which agree with the ratio $0 \cdot 65$ to $0 \cdot 35$ used in the more elaborate solutions, and confirms that the use of the $\frac{1}{4}/\frac{3}{4}$ approximation is exceedingly valuable in making a preliminary survey of any problem. It must be pointed out, however, that it is of limited use as it would not be possible to establish functions of which the main effect is to shift backwards the local aerodynamic centre. The effect of the rounding-off, as shown by a comparison of solutions 11 and 13, is to decrease the load coefficient at the median section by about 14 per cent, to shift back the local aerodynamic centre at the median section by 0·083 chord and the overall aerodynamic centre by $0 \cdot 04\bar{c}$, and to increase the induced drag factor from 1·107 to 1·157. The two simplified auxiliary solutions give an excellent approximation to the full 8-point solution. It has hitherto been accepted as good evidence of accuracy if the loading coefficient is in agreement for $\frac{1}{4}/\frac{3}{4}$ and the more complicated solutions. This criterion becomes less acceptable when the discontinuity is acute, as in the present case, and it is thought that differences are not necessarily due to inaccuracy, but may indicate that the $\frac{1}{4}/\frac{3}{4}$ solution is inadequate to represent the flow in the median region. The differences in C_{LL}/C_L for $\eta = 0$ between solutions 10 and 13, which are not serious and amount to a maximum of 4 per cent at $\eta = 0$, but do not exceed 2 per cent between $\eta = 0 \cdot 2$ and $0 \cdot 8$, do not, therefore, disprove the accuracy of the calculations.

6.3. *Rectangular wing: aspect ratio* 4*:* 0, 30, 45 *deg sweep-back.* *Tables* 19 *to* 24.
Rectangular wing: aspect ratio 2*:* 0, 30, 45 *deg sweep-back.* *Tables* 25 *to* 29.
Rectangular wing: aspect ratio 1*:* 0, 30, 45 *deg sweep-back.* *Tables* 30 *to* 34.

These wings have been calculated by the standard method, the 84-vortex pattern being used for the straight wings, and the 126 for those with sweep-back. The auxiliary loading functions used were as follows:—

A.R.4. $0 \cdot 65P_a + 0 \cdot 35P_b$

A.R.2. $0 \cdot 60P_a + 0 \cdot 40P_b$

A.R.1. $0 \cdot 50P_a + 0 \cdot 50P_b$

6.4. *Triangular wing,* 90 *deg apex angle, aspect ratio* 4 *and two other wings obtained by cropping the tips to aspect ratios* 3 *and* 2·309.—These wings have been calculated by the standard 126-vortex lattice, and the results are given in Tables 35 to 40.

The auxiliary function used for solutions 32 and 36 was $0 \cdot 65P_a + 0 \cdot 35P_b$.

6.5. A correction on $dc_L/d\alpha$ obtained by the 126-vortex lattice is sometimes required in order to bring it to the full potential value. It has not been possible to establish the factor for all cases, but figures derived from a delta and other wings suggest that the factor can be taken tentatively as independent of aspect ratio, and to vary as $1 + 0 \cdot 029$ (tangent of sweep-back of quarter-chord). All results given in the tables are uncorrected.

7. *Discussion of Results.*—A remarkable change in the solutions will be noted as the aspect ratio decreases. The loss in lift due to the centre-line correction is found to decrease with decreasing aspect ratio, while at the same time the induced drag decreases to the minimum of $(1/\pi A)\, c_L^2$ and the spanwise distribution of circulation approaches the elliptic form. The change is shown graphically in Fig. 3, in which are plotted the loading coefficient and local aerodynamic centre for sweep-back 0, 30 and 45 deg for wings of A.R.6 and A.R.1. The effect is independent of wing plan, as the triangular wings show precisely the same tendency. It does not necessarily follow that there is a possible saving in effort by assuming the elliptic distribution, as trial calculations with a 4-point solution for aspect ratio 1 show that the lift coefficient will be fairly accurately assessed, but the locus of local aerodynamic centres may be considerably in error unless the full number of control points are used.

8. *Comparison with Experiments.*—Some experimental results at a high Reynolds number for the three delta wings of section 6.2 taken from a report[6] issued by the Royal Aircraft Establishment, are given in Table 41 with the theoretical values. The values of $dc_L/d\alpha$ for the latter have

been multiplied by the correction factor 1·022, and it then appears that the wind-tunnel values for $dc_L/d\alpha$ are about 0·95 of the theoretical, and the measured aerodynamic centre does not vary by more than 0·017 mean chords from the theoretical. In view of the fact that the section t/c is about 10 per cent, these results must be regarded as very reasonable, although they are not intended to provide conclusive evidence as to the accuracy of the calculations.

9. *Acknowledgements*.—The writer desires to acknowledge the valuable assistance given by his colleague Mr. H. L. Nixon in some of the earlier work, by Miss D. E. Lehrian in the organisation of the latter stages of the work and by Misses S. D. Brown, W. M. Tafe and B. M. Skelton who took considerable responsibility in carrying out successfully the laborious task of computing the solutions.

REFERENCES

No.	*Author*	*Title, etc.*
1	V. M. Falkner	The Solution of Lifting Plane Problems by Vortex Lattice Theory. Report A.R.C. 10,895. (To be published).
2	V. M. Falkner	Appendix by E. J. Watson. Tables of Multhopp and Other Functions for Use in Lifting Line and Lifting Plane Theory. Report A.R.C. 11,234. (To be published).
3	V. M. Falkner	The Solution by Lifting Line Theory of Problems Involving Discontinuities. Report A.R.C. 10,922. (To be published).
4	H. Blenk	Der Eindecker als tragende Wirbelfläche. *Z.A.M.M.* Vol. 5. 1925.
5	V. M. Falkner	The Calculation of Aerodynamic Loading on Surfaces of Any Shape. R. & M. 1910. August, 1943.
6	R. Hills, R. C. Lock, and J. G. Ross	Interim Note on Wind-tunnel Tests of a Model Delta Wing. Report A.R.C. 10,535. (To be published).
7	E. N. Jacobs, K. M. Ward, and R. M. Pinkerton.	The Characteristics of the 78 Related Aerofoil Sections from Tests in the V.D. Tunnel. N.A.C.A. Report 460.
8	V. M. Falkner	The Use of Equivalent Slopes in Vortex Lattice Theory. R. & M. 2293. March, 1946.

APPENDIX

Calculation of Equivalent Slopes to represent the N.A.C.A. Camber-line

By

DORIS LEHRIAN, B.Sc.

If X be the distance from the leading edge in terms of the chord, and Y the distance in the direction normal to the line joining leading and trailing edges, in terms of the chord, the equation of the camber line is

$$Y = \frac{M}{P^2}(2PX - X^2) \text{ for } 0 \leqslant X \leqslant P.$$

and $$Y = \frac{M}{(1-P)^2}(1 - 2P + 2PX - X^2) \text{ for } P \leqslant X \leqslant 1$$

where M = maximum value of Y, at $X = P$.

For the three-term formula $k/2V = A_0 \cot \frac{1}{2}\Theta + A_1 \sin \Theta + A_2 \sin 2\Theta$ the equivalent slope is $A_0 - A_1 \cos \Theta - A_2 \cos 2\Theta$. The chordwise analysis for wing camber gives the solution

$$A_0 = -I_0 + \tfrac{3}{8}I_1 + \tfrac{1}{8}I_2$$

$$A_1 = \tfrac{1}{4}(I_1 - I_2)$$

$$A_2 = \tfrac{3}{4}(I_2 - I_1)$$

where $$I_0 = \frac{1}{\pi}\int_0^\pi \frac{dY}{dX} \cdot d\Theta, \; I_n = \frac{2}{\pi}\int_0^\pi \frac{dY}{dX} \cdot \cos n\Theta \, . \, d\Theta$$

and $$X = \tfrac{1}{2}(1 - \cos \Theta).$$

Applying this analysis to the N.A.C.A. camber line and writing $\Theta = \phi$ at $X = P$, $Y = M$, the integrals evaluate to

$$I_0 = \frac{16M \cos \phi \, (\sin \phi - \phi \cos \phi)}{\pi \, (1 - \cos^2 \phi)^2} - \frac{4M \cos \phi}{(1 + \cos \phi)^2}$$

$$I_1 = \frac{16M \cos \phi \, (\phi - \sin \phi \cos \phi)}{\pi \, (1 - \cos^2 \phi)^2} + \frac{4M}{(1 + \cos \phi)^2}$$

$$I_2 = \frac{32M \cos \phi}{3\pi \sin \phi}.$$

The values of A_0, A_1, A_2 are obtained immediately and the values of the equivalent slopes at the positions S_1 to S_9 are calculated for values of P equal to 0·2 (0·1) 0·7. These values are set out in Table A and are given in terms of the maximum value M.

For the two term formula $k/2V = A_0 \cot \frac{1}{2}\Theta + A_1 \sin \Theta$, the equivalent slope is $A_0 - A_1 \cos \Theta$. In this case the analysis for wing camber gives the solution

$$A_0 = -I_0 + \tfrac{1}{2}I_2$$

$$A_1 = I_1 - I_2$$

where the integrals I_0, I_1, I_2 have the same values as above. The equivalent slopes are calculated for the positions S_1 to S_9 for values of P equal to 0·2(0·1)0·7 and these values are set out in Table B.

TABLE A

Equivalent slopes to represent N.A.C.A. camber-line:—3-term formula

Slope	Position on chord-X	$P = 0\cdot2$	$P = 0\cdot3$	$P = 0\cdot4$	$P = 0\cdot5$	$P = 0\cdot6$	$P = 0\cdot7$
S_1	0	$2\cdot4522M$	$2\cdot7415M$	$3\cdot0809M$	$3\cdot5000M$	$4\cdot0500M$	$4\cdot8349M$
S_2	$0\cdot1\dot{6}$	0·6874	0·6058	0·5446	0·5000	0·4741	0·4765
S_3	0·25	0·0991	− 0·1060	− 0·3008	− 0·5000	− 0·7179	− 0·9763
S_4	$0\cdot3\dot{3}$	− 0·2931	− 0·5806	− 0·8644	− 1·1667	− 1·5125	− 1·9448
S_5	0·50	− 0·4892	− 0·8179	− 1·1462	− 1·5000	− 1·9098	− 2·4291
S_6	$0\cdot6\dot{6}$	0·0991	− 0·1060	− 0·3008	− 0·5000	− 0·7179	− 0·9763
S_7	0·75	0·6874	0·6058	0·5446	0·5000	0·4741	0·4765
S_8	$0\cdot8\dot{3}$	1·4717	1·5550	1·6718	1·8333	2·0634	2·4136
S_9	1·00	$3\cdot6287M$	$4\cdot1653M$	$4\cdot7717M$	$5\cdot5000M$	$6\cdot4339M$	$7\cdot7405M$

TABLE B

Equivalent slopes to represent N.A.C.A. camber line:—2-term formula

Slope	Position on chord-X	$P = 0\cdot2$	$P = 0\cdot3$	$P = 0\cdot4$	$P = 0\cdot5$	$P = 0\cdot6$	$P = 0\cdot7$
S_1	0	$-1\cdot9598M$	$-2\cdot5977M$	$-3\cdot2598M$	$-4\cdot0000M$	$-4\cdot8897M$	$-6\cdot0611M$
S_2	$0\cdot1\dot{6}$	− 1·1755	− 1·6485	− 2·1326	− 2·6667	− 3·3004	− 4·1240
S_3	0·25	− 0·7833	− 1·1739	− 1·5690	− 2·0000	− 2·5058	− 3·1555
S_4	$0\cdot3\dot{3}$	− 0·3911	− 0·6993	− 1·0053	− 1·3333	− 1·7112	− 2·1870
S_5	0·50	0·3932	0·2499	0·1219	0	− 0·1219	− 0·2499
S_6	$0\cdot6\dot{6}$	1·1776	1·1991	1·2491	1·3333	1·4674	1·6872
S_7	0·75	1·5698	1·6737	1·8127	2·0000	2·2620	2·6557
S_8	$0\cdot8\dot{3}$	1·9619	2·1483	2·3764	2·6667	3·0567	3·6242
S_9	1·00	$2\cdot7436M$	$3\cdot0975M$	$3\cdot5036M$	$4\cdot0000M$	$4\cdot6459M$	$5\cdot5613M$

TABLE 1

True and special values of P functions

η	P_a True	P_a 0·1 Lattice	P_a w/V	P_b True	P_b 0·1 Lattice	P_b w/V
0	0·14308	0·1578	1·0	0·24197	0·2518	1·00
0·05	0·12579		0·5	0·23047		0·75
0·10	0·09888	0·0940	0	0·20726	0·2092	0·50
0·15	0·08356		0	0·17952		0·25
0·20	0·07366	0·0726	0	0·15307	0·1493	0
0·25	0·06610		0	0·13523		0
0·30	0·05994	0·0594	0	0·12179	0·1206	0
0·35	0·05467		0	0·11067		0
0·40	0·05003	0·0497	0	0·10104	0·1004	0
0·45	0·04584		0	0·09244		0
0·50	0·04201	0·0418	0	0·08461	0·0841	0
0·55	0·03842		0	0·07731		0
0·60	0·03504	0·0349	0	0·07043	0·0701	0
0·65	0·03176		0	0·06380		0
0·70	0·02855	0·0284	0	0·05733	0·0571	0
0·75	0·02535		0	0·05089		0
0·80	0·02209	0·0220	0	0·04433	0·0442	0
0·85	0·01866		0	0·03744		0
0·90	0·01490	0·0149	0	0·02986	0·0299	0
0·95	0·01028		0	0·02064		0
0·9625	0·00887	0·0089	0	0·01778	0·0178	0
1·00	0		0	0		0
T_{15}	0·09992			0·19933		
T_{16}	0·50888			1·01517		
T_{19}	0·01599			0·03233		
T_{20}	0·03186			0·06388		

TABLE 2

Combinations of P functions

η	$P = 0{\cdot}65P_a + 0{\cdot}35P_b$			$P = 0{\cdot}60P_a + 0{\cdot}40P_b$			$P = 0{\cdot}50P_a + 0{\cdot}50P_b$		
	True	0·1 Lattice	w/V	True	0·1 Lattice	w/V	True	0·1 Lattice	w/V
0	0·17769	0·1907	1·0000	0·18264	0·1954	1·00	0·19252	0·2048	1·000
0·05	0·16243		0·5875	0·16766		0·60	0·17813		0·625
0·10	0·13681	0·1343	0·1750	0·14223	0·1401	0·20	0·15307	0·1516	0·250
0·15	0·11715		0·0875	0·12194		0·10	0·13154		0·125
0·20	0·10145	0·0994	0	0·10542	0·1033	0	0·11336	0·1109	0
0·25	0·09030		0	0·09375		0	0·10066		0
0·30	0·08159	0·0808	0	0·08468	0·0839	0	0·09086	0·0900	0
0·35	0·07427		0	0·07707		0	0·08267		0
0·40	0·06788	0·0674	0	0·07043	0·0700	0	0·07554	0·0750	0
0·45	0·06215		0	0·06448		0	0·06914		0
0·50	0·05692	0·0566	0	0·05905	0·0587	0	0·06331	0·0630	0
0·55	0·05203		0	0·05398		0	0·05786		0
0·60	0·04743	0·0472	0	0·04920	0·0490	0	0·05274	0·0525	0
0·65	0·04297		0	0·04458		0	0·04778		0
0·70	0·03862	0·0385	0	0·04006	0·0399	0	0·04294	0·0428	0
0·75	0·03429		0	0·03557		0	0·03812		0
0·80	0·02987	0·0298	0	0·03099	0·0309	0	0·03321	0·0331	0
0·85	0·02523		0	0·02617		0	0·02805		0
0·90	0·02014	0·0201	0	0·02088	0·0209	0	0·02238	0·0224	0
0·95	0·01391		0	0·01442		0	0·01546		0
0·9625	0·01199	0·0120	0	0·01243	0·0124	0	0·01332	0·0133	0
1·00	0		0	0		0	0		0
T_{15}	0·13471			0·13968			0·14962		
T_{16}	0·68608			0·71140			0·76202		
T_{19}	0·02171			0·02253			0·02416		
T_{20}	0·04307			0·04467			0·04787		

TABLE 3

True and special values of P functions

η	P_1			P_2			P_3		
	True	0·1 Lattice	w/V	True	0·1 Lattice	w/V	True	0·1 Lattice	w/V
0	0·19778	0·1881	0	0·14730	0·1451	0	0·11987	0·1188	0
0·05	0·20936		0·5	0·14966		0	0·12078		0
0·10	0·21675	0·2303	1·0	0·15883	0·1535	0	0·12372	0·1223	0
0·15	0·19191		0·5	0·18047		0·5	0·12949		0
0·20	0·15884	0·1535	0	0·19316	0·2075	1·0	0·14104	0·1360	0
0·25	0·13826		0	0·17172		0·5	0·16446		0·5
0·30	0·12371	0·1223	0	0·14103	0·1360	0	0·17847	0·1930	1·0
0·35	0·11200		0	0·12218		0	0·15806		0·5
0·40	0·10201	0·1013	0	0·10897	0·1077	0	0·12815	0·1232	0
0·45	0·09320		0	0·09824		0	0·10993		0
0·50	0·08519	0·0847	0	0·08900	0·0884	0	0·09717	0·0960	0
0·55	0·07778		0	0·08075		0	0·08678		0
0·60	0·07079	0·0705	0	0·07314	0·0727	0	0·07776	0·0772	0
0·65	0·06409		0	0·06598		0	0·06957		0
0·70	0·05757	0·0573	0	0·05906	0·0588	0	0·06191	0·0616	0
0·75	0·05109		0	0·05228		0	0·05452		0
0·80	0·04448	0·0444	0	0·04542	0·0453	0	0·04720	0·0470	0
0·85	0·03757		0	0·03829		0	0·03964		0
0·90	0·02992	0·0300	0	0·03048	0·0305	0	0·03147	0·0315	0
0·95	0·02071		0	0·02104		0	0·02167		0
0·9625	0·01783	0·0178	0	0·01811	0·0181	0	0·01865	0·0187	0
1·00	0		0	0		0	0		0
T_{15}	0·19882			0·19578			0·19059		
T_{16}	1·01260			0·99712			0·97068		
T_{19}	0·03268			0·03412			0·03572		
T_{20}	0·06405			0·06502			0·06683		

TABLE 3—*continued*

True and special values of P functions

η	P_4			P_5			P_6		
	True	0·1 Lattice	w/V	True	0·1 Lattice	w/V	True	0·1 Lattice	w/V
0	0·10004	0·0994	0	0·08401	0·0836	0	0·07002	0·0698	0
0·05	0·10053		0	0·08428		0	0·07021		0
0·10	0·10200	0·1013	0	0·08516	0·0847	0	0·07076	0·0705	0
0·15	0·10468		0	0·08669		0	0·07171		0
0·20	0·10896	0·1077	0	0·08900	0·0884	0	0·07312	0·0728	0
0·25	0·11576		0	0·09235		0	0·07506		0
0·30	0·12814	0·1232	0	0·09715	0·0960	0	0·07772	0·0772	0
0·35	0·15220		0·5	0·10437		0	0·08130		0
0·40	0·16672	0·1813	1·0	0·11704	0·1122	0	0·08628	0·0852	0
0·45	0·14669		0·5	0·14132		0·5	0·09362		0
0·50	0·11705	0·1122	0	0·15598	0·1707	1·0	0·10632	0·1015	0
0·55	0·09900		0	0·13600		0·5	0·13056		0·5
0·60	0·08631	0·0852	0	0·10633	0·1015	0	0·14511	0·1599	1·0
0·65	0·07588		0	0·08815		0	0·12491		0·5
0·70	0·06668	0·0662	0	0·07522	0·0742	0	0·09491	0·0902	0
0·75	0·05819		0	0·06439		0	0·07623		0
0·80	0·05000	0·0498	0	0·05458	0·0542	0	0·06256	0·0617	0
0·85	0·04178		0	0·04512		0	0·05066		0
0·90	0·03298	0·0330	0	0·03537	0·0353	0	0·03911	0·0391	0
0·95	0·02263		0	0·02410		0	0·02635		0
0·9625	0·01945	0·0195	0	0·02069	0·0207	0	0·02257	0·0226	0
1·00	0		0	0		0	0		0
T_{15}	0·18309			0·17294			0·15967		
T_{16}	0·93248			0·88080			0·81320		
T_{19}	0·03711			0·03797			0·03794		
T_{20}	0·06957			0·07368			0·07985		

TABLE 3—*continued*

True and special values of P functions

η	P_7		
	True	0·1 Lattice	w/V
0	0·05701	0·0570	0
0·05	0·05713		0
0·10	0·05749	0·0575	0
0·15	0·05810		0
0·20	0·05900	0·0590	0
0·25	0·06022		0
0·30	0·06182	0·0617	0
0·35	0·06392		0
0·40	0·06663	0·0664	0
0·45	0·07022		0
0·50	0·07515	0·0744	0
0·55	0·08236		0
0·60	0·09486	0·0904	0
0·65	0·11879		0·5
0·70	0·13290	0·1481	1·0
0·75	0·11210		0·5
0·80	0·08127	0·0771	0
0·85	0·06134		0
0·90	0·04571	0·0457	0
0·95	0·03010		0
0·9625	0·02566	0·0257	0
1·00	0		0
T_{15}	0·14237		
T_{16}	0·72506		
T_{19}	0·03653		
T_{20}	0·08974		

TABLE 4

Calculation of induced drag for Solution 7

$$\left(\frac{w}{V}\right) \text{Fourier} = \frac{\Sigma n A_n \sin n\phi}{\sin \phi}$$

$$\text{where } A_1 = \pi\,(a_0 + 0\cdot5a_1 + 0\cdot25c_0 + 0\cdot125c_1 + 0\cdot125e_0 + 0\cdot0625e_1)$$

$$A_3 = \pi\,(0\cdot25c_0 + 0\cdot125c_1 + 0\cdot1875e_0 + 0\cdot09375e_1)$$

$$A_5 = \pi\,(0\cdot0625e_0 + 0\cdot03125e_1)$$

w/V for P function $= \pi\,(-\ 0\cdot05183)\ (w/V)_P$ where $(w/V)_P$ is the induced downwash due to $K/4sV = P$.

η	$K/4sV$	w/V Fourier	w/V P function	Total w/V	$(K/4sV) \times (w/V)$	Factors
0	0·1623	0·1354	− 0·1628	− 0·0274	− 0·0044	1
0·05	0·1648	0·1362	− 0·0957	0·0405	0·0067	4
0·10	0·1690	0·1386	− 0·0285	0·1101	0·0186	2
0·15	0·1724	0·1425	− 0·0142	0·1283	0·0221	4
0·20	0·1751	0·1480	0	0·1480	0·0259	2
0·25	0·1771	0·1552	0	0·1552	0·0275	4
0·30	0·1785	0·1640	0	0·1640	0·0293	2
0·35	0·1796	0·1745	0	0·1745	0·0313	4
0·40	0·1804	0·1867	0	0·1867	0·0337	2
0·45	0·1807	0·2007	0	0·2007	0·0363	4
0·50	0·1805	0·2166	0	0·2166	0·0391	2
0·55	0·1795	0·2344	0	0·2344	0·0421	4
0·60	0·1776	0·2543	0	0·2543	0·0452	2
0·65	0·1746	0·2762	0	0·2762	0·0482	4
0·70	0·1701	0·3003	0	0·3003	0·0511	2
0·75	0·1635	0·3266	0	0·3266	0·0534	4
0·80	0·1541	0·3554	0	0·3554	0·0548	2
0·85	0·1408	0·3867	0	0·3867	0·0544	4
0·90	0·1213	0·4205	0	0·4205	0·0510	1·800
0·95	0·0906	0·4572	0	0·4572	0·0414	4·525
1·00	0	0·4967	0	0·4967	0	0·675

$$C_{DI} = \frac{16s^2}{S}\,\frac{Integral}{60} = 1\cdot082\,\frac{1}{\pi A}\,C_L{}^2.$$

TABLE 5

Solution 1

Rectangular wing, aspect ratio 6, 84 *vortex* 9-*point solution*

a_0	$0 \cdot 06811$	c_0	$0 \cdot 01638$	e_0	$0 \cdot 02716$
a_1	$-0 \cdot 00197$	c_1	$-0 \cdot 00155$	e_1	$-0 \cdot 03698$
a_2	$-0 \cdot 00057$	c_2	$0 \cdot 00444$	e_2	$-0 \cdot 01369$

$$dc_L/d\alpha = 4 \cdot 270 \qquad C_{DI} = 1 \cdot 018 \frac{1}{\pi A} C_L^2$$

Aerodynamic centre $0 \cdot 2399\bar{c}$ behind leading edge.

Loading

η	C_{LL}/C_L	Local a.c.	η	C_{LL}/C_L	Local a.c.
0	1·185	0·247	0·55	1·071	0·241
0·05	1·184	0·247	0·60	1·044	0·239
0·10	1·182	0·247	0·65	1·010	0·237
0·15	1·178	0·247	0·70	0·969	0·234
0·20	1·172	0·247	0·75	0·919	0·231
0·25	1·165	0·247	0·80	0·855	0·227
0·30	1·156	0·246	0·85	0·772	0·223
0·35	1·144	0·246	0·90	0·658	0·218
0·40	1·130	0·245	0·95	0·487	0·214
0·45	1·114	0·244	1·00	0	0·208
0·50	1·094	0·242			

Induced camber

Position on chord	Spanwise location: value of η			
	0	0·8	0·9	0·95
0	0	0	0	0
0·1	− 0·001	− 0·003	− 0·004	− 0·003
0·2	− 0·001	− 0·006	− 0·006	− 0·006
0·3	− 0·001	− 0·007	− 0·008	− 0·007
0·4	− 0·001	− 0·008	− 0·008	− 0·008
0·5	− 0·001	− 0·008	− 0·008	− 0·007
0·6	− 0·001	− 0·007	− 0·008	− 0·007
0·7	− 0·001	− 0·006	− 0·006	− 0·005
0·8	− 0·001	− 0·004	− 0·004	− 0·004
0·9	0	− 0·002	− 0·002	− 0·002
1·0	0	0	0	0

Local a.c. = Local aerodynamic centre.

TABLE 6

Solution 2

Rectangular wing, aspect ratio 6, 84 *vortex* 6-*point solution*

a_0	0.06759	c_0	0.01933	e_0	0.01738
a_1	-0.00140	c_1	-0.00654	e_1	-0.02168

$$dc_L/d\alpha = 4.247 \qquad C_{DI} = 1.016 \frac{1}{\pi A} C_L^2$$

Aerodynamic centre $0.2400\bar{c}$ behind leading edge.

Loading

η	C_{LL}/C_L	Local a.c.	η	C_{LL}/C_L	Local a.c.
0	1·188	0·247	0·55	1·073	0·241
0·05	1·187	0·247	0·60	1·044	0·239
0·10	1·184	0·247	0·65	1·010	0·236
0·15	1·180	0·247	0·70	0·968	0·234
0·20	1·175	0·247	0·75	0·916	0·231
0·25	1·168	0·246	0·80	0·851	0·227
0·30	1·158	0·246	0·85	0·766	0·223
0·35	1·147	0·245	0·90	0·652	0·219
0·40	1·133	0·245	0·95	0·481	0·214
0·45	1·116	0·244	1·00	0	0·209
0·50	1·096	0·242			

Induced camber

Position on chord	Spanwise location: value of η			
	0	0·8	0·9	0·95
0	0	0	0	0
0·1	0	− 0·002	− 0·002	− 0·002
0·2	− 0·001	− 0·004	− 0·004	− 0·004
0·3	− 0·001	− 0·005	− 0·005	− 0·005
0·4	− 0·001	− 0·006	− 0·006	− 0·005
0·5	− 0·001	− 0·006	− 0·006	− 0·006
0·6	− 0·001	− 0·006	− 0·006	− 0·005
0·7	− 0·001	− 0·005	− 0·005	− 0·005
0·8	− 0·001	− 0·004	− 0·004	− 0·004
0·9	0	− 0·002	− 0·002	− 0·002
1·0	0	0	0	0

TABLE 7

Solution 3

Rectangular wing, aspect ratio 6, *Blenk's* 6-*point solution, with* $\eta = 0 \cdot 2$ *and* $0 \cdot 8$, *revised by Argyris*

a_0	$0 \cdot 06713$	c_0	$0 \cdot 03196$
a_1	$-0 \cdot 00156$	c_1	$-0 \cdot 02312$
a_2	$0 \cdot 00009$	c_2	$-0 \cdot 00474$

$$dc_L/d\alpha = 4 \cdot 231 \qquad C_{DI} = 1 \cdot 015 \frac{1}{\pi A} C_L^2$$

Aerodynamic centre $0 \cdot 2391 \bar{c}$ behind leading edge.

η	C_{LL}/C_L	Local a.c.	η	C_{LL}/C_L	Local a.c.
0	1·182	0·247	0·55	1·079	0·238
0·05	1·182	0·247	0·60	1·051	0·236
0·10	1·180	0·247	0·65	1·015	0·234
0·15	1·177	0·246	0·70	0·972	0·233
0·20	1·173	0·246	0·75	0·917	0·231
0·25	1·167	0·245	0·80	0·849	0·229
0·30	1·159	0·244	0·85	0·761	0·227
0·35	1·149	0·243	0·90	0·644	0·225
0·40	1·137	0·242	0·95	0·472	0·223
0·45	1·122	0·240	1·00	0	0·221
0·50	1·103	0·239			

TABLE 8

Solution 4

Rectangular wing, aspect ratio 6, 4-*term lifting-line solution*

$$K/4sV = 0\cdot2402 \sin \Theta + 0\cdot0289 \sin 3\Theta + 0\cdot0057 \sin 5\Theta + 0\cdot0010 \sin 7\Theta$$

$$dc_L/d\alpha = 4\cdot527 \qquad C_{DI} = 1\cdot046 \frac{1}{\pi A} C_L^2$$

Local and overall aerodynamic centre $0\cdot25$ chord.

η	C_{LL}	η	C_{LL}
0	1·145	0·6	1·043
0·1	1·143	0·7	0·988
0·2	1·137	0·8	0·900
0·3	1·125	0·9	0·728
0·4	1·107	1·0	0
0·5	1·081		

TABLE 9

Solution 5

Rectangular wing, aspect ratio 6, 84-*vortex* 9-*point solutions for wing with N.A.C.A. camber, at zero lift, based on equivalent slopes*

C_{m0} and α_0 are given in terms of the maximum camber M, which is located at a ratio P of the chord.

P	A.R.6.		A.R. infinity	
	α_0	C_{m0}	α_0	C_{m0}
0·2	− 1·633	− 1·748	− 1·570	− 1·848
0·3	− 1·750	− 2·115	− 1·674	− 2·236
0·4	− 1·904	− 2·512	− 1·813	− 2·656
0·5	− 2·108	− 2·972	− 2·000	− 3·142
0·6	− 2·390	− 3·542	− 2·262	− 3·745
0·7	− 2·812	− 4·317	− 2·656	− 4·564

TABLE 10

Solution 6

Constant-chord wing, aspect ratio 6, 30 *deg sweep-back,* 126-*vortex* 6-*point standard solution*

a_0	$0 \cdot 05703$	c_0	$0 \cdot 03557$	e_0	$0 \cdot 03123$
a_1	$0 \cdot 00136$	c_1	$-0 \cdot 00172$	e_1	$-0 \cdot 05625$

$$dc_L/d\alpha = 3 \cdot 955 \qquad C_{DI} = 1 \cdot 058 \frac{1}{\pi A} C_L^2$$

Aerodynamic centre $1 \cdot 035\bar{c}$ behind apex.

Loading

η	C_{LL}/C_L	Local a.c.	η	C_{LL}/C_L	Local a.c.
0	1·100	0·253	0·55	1·091	0·242
0·05	1·101	0·253	0·60	1·077	0·238
0·10	1·101	0·253	0·65	1·057	0·234
0·15	1·103	0·253	0·70	1·027	0·228
0·20	1·104	0·252	0·75	0·986	0·222
0·25	1·106	0·252	0·80	0·929	0·215
0·30	1·107	0·252	0·85	0·848	0·207
0·35	1·107	0·251	0·90	0·730	0·198
0·40	1·107	0·249	0·95	0·545	0·187
0·45	1·104	0·248	1·00	0	0·176
0·50	1·099	0·245			

Induced camber

Position on chord	Spanwise location: value of η			
	0	0·8	0·9	0·95
0	0·000	0·000	0·000	0·000
0·1	0·000	− 0·004	− 0·004	− 0·004
0·2	0·001	− 0·007	− 0·008	− 0·007
0·3	0·001	− 0·009	− 0·010	− 0·009
0·4	0·001	− 0·010	− 0·012	− 0·010
0·5	0·001	− 0·010	− 0·012	− 0·011
0·6	0·001	− 0·010	− 0·012	− 0·010
0·7	0·001	− 0·009	− 0·010	− 0·009
0·8	0·001	− 0·007	− 0·008	− 0·007
0·9	0·000	− 0·004	− 0·004	− 0·004
1·0	0·000	0·000	0·000	0·000

TABLE 11

Solution 7

Constant chord wing, aspect ratio 6, 30 *deg sweep-back,* 126-*vortex* 6-*point standard solution modified*

Auxiliary solution:—

a_0' 0·01583 p_0 − 0·18500

a_1' − 0·02537 p_1 0·26634

$$dc_L/d\alpha = 3{\cdot}877 \qquad C_{DI} = 1{\cdot}082 \frac{1}{\pi A} C_L^2$$

Aerodynamic centre $1{\cdot}053\bar{c}$ behind apex.

Loading

η	C_{LL}/C_L	Local a.c.	η	C_{LL}/C_L	Local a.c.
0	1·004	0·306	0·55	1·111	0·242
0·05	1·020	0·296	0·60	1·100	0·238
0·10	1·046	0·279	0·65	1·081	0·234
0·15	1·067	0·267	0·70	1·053	0·228
0·20	1·084	0·257	0·75	1·012	0·222
0·25	1·096	0·252	0·80	0·954	0·215
0·30	1·105	0·252	0·85	0·872	0·207
0·35	1·112	0·251	0·90	0·751	0·198
0·40	1·117	0·249	0·95	0·561	0·187
0·45	1·118	0·248	1·00	0	0·176
0·50	1·117	0·245			

Induced camber

Position on chord	Spanwise location: value of η			
	0	0·8	0·9	0·95
0	0	0	0	0
0·1	0·006	− 0·006	− 0·006	− 0·005
0·2	0·012	− 0·010	− 0·011	− 0·009
0·3	0·015	− 0·014	− 0·014	− 0·012
0·4	0·017	− 0·016	− 0·016	− 0·014
0·5	0·018	− 0·016	− 0·017	− 0·014
0·6	0·017	− 0·016	− 0·016	− 0·014
0·7	0·015	− 0·014	− 0·014	− 0·012
0·8	0·012	− 0·010	− 0·011	− 0·009
0·9	0·006	− 0·006	− 0·006	− 0·005
1·0	0	0	0	0

TABLE 12

Solution 8

Constant chord wing, aspect ratio 6, 45 *deg sweep-back*, 21-*vortex standard solution:* 3 *control points at* $\eta = 0{\cdot}2,\ 0{\cdot}6,\ 0{\cdot}8$

a_0 0·04686 $dc_L/d\alpha = 3{\cdot}323$

c_0 0·03035 $C_{DI} = 1{\cdot}098 \dfrac{1}{\pi A} C_L^2$

e_0 0·01329 Local aerodynamic centre 0·25 chord.

η	C_{LL}/C_L	η	C_{LL}/C_L
0	1·063	0·6	1·080
0·1	1·065	0·7	1·052
0·2	1·069	0·8	0·977
0·3	1·076	0·9	0·793
0·4	1·083	0·95	0·602
0·5	1·086	1·0	0

TABLE 13

Solution 9

Constant chord wing, aspect ratio 6, 45 *deg sweep-back*, 21-*vortex standard solution:* 4 *control points at* $\eta = 0{\cdot}2,\ 0{\cdot}4,\ 0{\cdot}6,\ 0{\cdot}8$

a_0 0·04709 $dc_L/d\alpha = 3{\cdot}339$

c_0 0·03197 $C_{DI} = 1{\cdot}094 \dfrac{1}{\pi A} C_L^2$

e_0 0·01037 Local aerodynamic centre 0·25 chord.

η	C_{LL}/C_L	η	C_{LL}/C_L
0	1·064	0·6	1·083
0·1	1·065	0·7	1·052
0·2	1·071	0·8	0·973
0·3	1·078	0·9	0·786
0·4	1·086	0·95	0·595
0·5	1·090	1·0	0

TABLE 14

Solution 10

Constant chord wing, aspect ratio 6, 45 *deg sweep-back,* 21-*vortex solution:* 6 *control points at* $\eta = 0, 0\cdot1, 0\cdot2, 0\cdot4, 0\cdot6, 0\cdot8$

a_0	$0\cdot05071$	p_{0a}	$-0\cdot03990$
c_0	$0\cdot02797$	p_{0b}	$-0\cdot02105$
e_0	$0\cdot01326$		

$dc_L/d\alpha = 3\cdot207$ $\quad C_{DI} = 1\cdot131 \dfrac{1}{\pi A} C_L^2$ $\quad$ Local aerodynamic centre $0\cdot25$ chord.

η	C_{LL}/C_L	η	C_{LL}/C_L
0	0·938	0·6	1·108
0·1	0·997	0·7	1·080
0·2	1·050	0·8	1·002
0·3	1·080	0·9	0·812
0·4	1·100	0·95	0·617
0·5	1·110	1·0	0

TABLE 15

Solution 11

Constant chord wing, aspect ratio 6, 45 *deg sweep-back,* 126-*vortex* 6-*point standard solution:* $\eta = 0{\cdot}2,\ 0{\cdot}6,\ 0{\cdot}8$

a_0	$0{\cdot}04734$	c_1	$0{\cdot}01354$	$dc_L/d\alpha = 3{\cdot}464$	
a_1	$0{\cdot}00184$	e_0	$0{\cdot}04771$	$C_{DI} = 1{\cdot}107 \dfrac{1}{\pi A} C_L^2$	
c_0	$0{\cdot}02800$	e_1	$-\ 0{\cdot}07056$		

Aerodynamic centre $1{\cdot}657\bar{c}$ behind apex.

Loading

η	C_{LL}/C_L	Local a.c.	η	C_{LL}/C_L	Local a.c.
0	1·050	0·255	0·55	1·089	0·249
0·05	1·051	0·255	0·60	1·086	0·245
0·10	1·052	0·255	0·65	1·078	0·240
0·15	1·055	0·255	0·70	1·061	0·234
0·20	1·059	0·256	0·75	1·033	0·228
0·25	1·064	0·256	0·80	0·987	0·220
0·30	1·069	0·256	0·85	0·916	0·211
0·35	1·074	0·256	0·90	0·802	0·200
0·40	1·080	0·255	0·95	0·610	0·190
0·45	1·085	0·254	1·00	0	0·178
0·50	1·088	0·252			

Induced camber

Position on chord	Spanwise location: value of η			
	0	0·8	0·9	0·95
0	0	0	0	0
0·1	0·001	− 0·003	− 0·004	− 0·004
0·2	0·001	− 0·006	− 0·008	− 0·008
0·3	0·001	− 0·008	− 0·011	− 0·010
0·4	0·002	− 0·009	− 0·012	− 0·011
0·5	0·002	− 0·010	− 0·013	− 0·012
0·6	0·002	− 0·009	− 0·012	− 0·011
0·7	0·001	− 0·008	− 0·011	− 0·010
0·8	0·001	− 0·006	− 0·008	− 0·008
0·9	0·001	− 0·003	− 0·004	− 0·004
1·0	0	0	0	0

TABLE 16

Solution 12

Constant chord wing, aspect ratio 6, 45 *deg sweep-back,* 126-*vortex standard solution modified by* 6 *variable* 6-*point auxiliary solution*

a_0'	0·01512	p_{0a}	− 0·24688	p_{0b}	− 0·00216
a_1'	− 0·02176	p_{1a}	0·39712	p_{1b}	− 0·04012

$$dc_L/d\alpha = 3 \cdot 367$$

η	C_{LL}/C_L	Local a.c.	η	C_{LL}/C_L	Local a.c.
0	0·900	0·335	0·50	1·114	0·252
0·05	0·925	0·313	0·60	1·121	0·245
0·10	0·968	0·283	0·70	1·100	0·234
0·15	1·000	0·268	0·80	1·027	0·220
0·20	1·027	0·261	0·90	0·836	0·200
0·25	1·048	0·256	0·95	0·636	0·190
0·30	1·065	0·256	1·00	0	0·178
0·40	1·094	0·255			

TABLE 17

Solution 13

Constant chord wing, aspect ratio 6, 45 *deg sweep-back,* 126-*vortex* 8-*point solution:* $\eta = 0, 0{\cdot}2, 0{\cdot}6, 0{\cdot}8$

a_0	$0{\cdot}06977$	e_0	$0{\cdot}07542$	$dc_L/d\alpha = 3{\cdot}304$
a_1	$-0{\cdot}03426$	e_1	$-0{\cdot}11816$	$C_{DI} = 1{\cdot}157 \dfrac{1}{\pi A} C_L^2$
c_0	$-0{\cdot}00719$	p_0	$-0{\cdot}24857$	
c_1	$0{\cdot}07404$	p_1	$0{\cdot}34940$	

Aerodynamic centre $1{\cdot}697\bar{c}$ behind apex.

Loading

η	C_{LL}/C_L	Local a.c.	η	C_{LL}/C_L	Local a.c.
0	0·902	0·338	0·55	1·116	0·248
0·05	0·928	0·320	0·60	1·116	0·246
0·10	0·971	0·292	0·65	1·109	0·242
0·15	1·005	0·274	0·70	1·095	0·236
0·20	1·033	0·263	0·75	1·068	0·229
0·25	1·053	0·257	0·80	1·023	0·220
0·30	1·069	0·253	0·85	0·952	0·209
0·35	1·083	0·252	0·90	0·836	0·197
0·40	1·095	0·251	0·95	0·638	0·183
0·45	1·105	0·250	1·00	0	0·167
0·50	1·112	0·250			

Induced camber

Position on chord	Spanwise location: value of η			
	0	0·8	0·9	0·95
0	0	0	0	0
0·1	0·009	− 0·004	− 0·005	− 0·005
0·2	0·016	− 0·006	− 0·009	− 0·009
0·3	0·021	− 0·008	− 0·012	− 0·012
0·4	0·024	− 0·009	− 0·014	− 0·013
0·5	0·025	− 0·010	− 0·014	− 0·014
0·6	0·024	− 0·009	− 0·014	− 0·013
0·7	0·021	− 0·008	− 0·012	− 0·012
0·8	0·016	− 0·006	− 0·009	− 0·009
0·9	0·009	− 0·004	− 0·005	− 0·005
1·0	0	0	0	0

TABLE 18

Solution 14

Constant chord wing, aspect ratio 6, 45 *deg sweep-back,* 126*-vortex standard solution modified by* 4 *variable* 4*-point auxiliary solution*

a_0'	$0 \cdot 02010$	p_0	$-0 \cdot 23686$	$dc_L/d\alpha = 3 \cdot 365$	
a_1'	$-0 \cdot 03061$	p_1	$0 \cdot 32271$		

η	C_{LL}/C_L	Local a.c.	η	C_{LL}/C_L	Local a.c.
0	0·888	0·340	0·50	1·117	0·252
0·05	0·914	0·323	0·60	1·124	0·245
0·10	0·959	0·296	0·70	1·104	0·234
0·15	0·994	0·277	0·80	1·030	0·220
0·20	1·024	0·264	0·90	0·839	0·200
0·25	1·046	0·256	0·95	0·638	0·190
0·30	1·065	0·256	1·00	0	0·178
0·40	1·095	0·255			

TABLE 19

Solution 15

Rectangular wing, aspect ratio 4, 84*-vortex,* 6*-point solution:* $\eta = 0 \cdot 2,\ 0 \cdot 6,\ 0 \cdot 8$

a_0	$0 \cdot 09213$	c_1	$-0 \cdot 00535$	$dc_L/d\alpha = 3 \cdot 639$	
a_1	$-0 \cdot 00799$	e_0	$0 \cdot 02116$	$C_{DI} = 1 \cdot 006 \dfrac{1}{\pi A} C_L^2$	
c_0	$0 \cdot 01880$	e_1	$-0 \cdot 04195$		

Aerodynamic centre $0 \cdot 2302\bar{c}$ behind leading edge.

η	C_{LL}/C_L	Local a.c.	η	C_{LL}/C_L	Local a.c.
0	1·217	0·239	0·55	1·073	0·232
0·05	1·216	0·239	0·60	1·038	0·230
0·10	1·213	0·239	0·65	0·997	0·227
0·15	1·208	0·238	0·70	0·948	0·223
0·20	1·201	0·238	0·75	0·888	0·219
0·25	1·192	0·238	0·80	0·816	0·214
0·30	1·180	0·238	0·85	0·727	0·208
0·35	1·166	0·237	0·90	0·610	0·201
0·40	1·148	0·236	0·95	0·444	0·193
0·45	1·127	0·235	1·00	0	0·184
0·50	1·102	0·234			

TABLE 20

Solution 16

Constant chord wing, aspect ratio 4, 30 *deg sweep-back,* 126-*vortex* 6-*point standard solution:* $\eta = 0\cdot2,\ 0\cdot6,\ 0\cdot8$

a_0	$0\cdot07722$	c_1	$-\,0\cdot03666$	$dc_L/d\alpha = 3\cdot467$	
a_1	$0\cdot00331$	e_0	$0\cdot01921$	$C_{DI} = 1\cdot027 \dfrac{1}{\pi A} C_L^2$	
c_0	$0\cdot05918$	e_1	$-\,0\cdot05885$		

Aerodynamic centre $0\cdot750\bar{c}$ behind apex.

η	C_{LL}/C_L	Local a.c.	η	$C/_{LL}C_L$	Local a.c.
0	1·144	0·255	0·55	1·093	0·232
0·05	1·144	0·255	0·60	1·070	0·226
0·10	1·144	0·255	0·65	1·039	0·220
0·15	1·144	0·254	0·70	0·998	0·213
0·20	1·143	0·253	0·75	0·946	0·204
0·25	1·142	0·251	0·80	0·877	0·195
0·30	1·140	0·249	0·85	0·787	0·185
0·35	1·137	0·247	0·90	0·665	0·173
0·40	1·131	0·244	0·95	0·486	0·160
0·45	1·123	0·241	1·00	0	0·145
0·50	1·110	0·237			

TABLE 21

Solution 17

Constant-chord wing, aspect ratio 4, 30 *deg sweep-back,* 126-*vortex* 6-*point standard solution modified by* 4-*point auxiliary solution*

a_0'	$0\cdot01804$	p_0	$-\,0\cdot21921$	$dc_L/d\alpha = 3\cdot400$
a_1'	$-\,0\cdot03130$	p_1	$0\cdot34336$	$C_{DI} = 1\cdot040 \dfrac{1}{\pi A} C_L^2$

Aerodynamic centre $0\cdot762\bar{c}$ behind apex.

η	C_{LL}/C_L	Local a.c.	η	C_{LL}/C_L	Local a.c.
0	1·076	0·307	0·55	1·108	0·232
0·05	1·087	0·297	0·60	1·086	0·226
0·10	1·105	0·281	0·65	1·056	0·220
0·15	1·119	0·269	0·70	1·016	0·213
0·20	1·129	0·260	0·75	0·964	0·204
0·25	1·136	0·252	0·80	0·894	0·195
0·30	1·139	0·249	0·85	0·804	0·185
0·35	1·140	0·247	0·90	0·679	0·173
0·40	1·138	0·244	0·95	0·497	0·160
0·45	1·133	0·241	1·00	0	0·145
0·50	1·123	0·237			

TABLE 22

Solution 18

Constant-chord wing, aspect ratio 4, 45 *deg sweep-back,* 126-*point vortex* 6-*point standard solution:* $\eta = 0 \cdot 2,\ 0 \cdot 6,\ 0 \cdot 8$

a_0	$0 \cdot 06463$	c_1	$-0 \cdot 00344$	$dc_L/d\alpha$	$= 3 \cdot 121$
a_1	$0 \cdot 00530$	e_0	$0 \cdot 04759$	C_{DI}	$= 1 \cdot 061 \dfrac{1}{\pi A} C_L^2$
c_0	$0 \cdot 05306$	e_1	$-0 \cdot 11200$		

Aerodynamics centre $1 \cdot 157\bar{c}$ behind apex.

η	C_{LL}/C_L	Local a.c.	η	C_{LL}/C_L	Local a.c.
0	1·084	0·260	0·55	1·104	0·241
0·05	1·084	0·260	0·60	1·091	0·235
0·10	1·086	0·260	0·65	1·070	0·227
0·15	1·090	0·259	0·70	1·040	0·218
0·20	1·094	0·259	0·75	0·996	0·207
0·25	1·098	0·258	0·80	0·934	0·195
0·30	1·104	0·257	0·85	0·848	0·180
0·35	1·108	0·255	0·90	0·726	0·164
0·40	1·111	0·253	0·95	0·537	0·146
0·45	1·112	0·250	1·00	0	0·125
0·50	1·110	0·246			

TABLE 23

Solution 19

Constant-chord wing, aspect ratio 4, 45 *deg sweep-back,* 126-*vortex* 8-*point solution:* $\eta = 0,\ 0 \cdot 2,\ 0 \cdot 6,\ 0 \cdot 8$

a_0	$0 \cdot 09138$	e_0	$0 \cdot 07958$	$dc_L/d\alpha$	$= 2 \cdot 986$
a_1	$-0 \cdot 04157$	e_1	$-0 \cdot 16959$	C_{DI}	$= 1 \cdot 092 \dfrac{1}{\pi A} C_L^2$
c_0	$0 \cdot 01219$	p_0	$-0 \cdot 30843$		
c_1	$0 \cdot 07073$	p_1	$0 \cdot 47236$		

Aerodynamic centre $1 \cdot 182\bar{c}$ behind apex.

η	C_{LL}/C_L	Local a.c.	η	C_{LL}/C_L	Local a.c.
0	0·972	0·342	0·55	1·125	0·240
0·05	0·991	0·325	0·60	1·114	0·235
0·10	1·024	0·299	0·65	1·096	0·228
0·15	1·050	0·282	0·70	1·067	0·219
0·20	1·072	0·269	0·75	1·024	0·208
0·25	1·089	0·262	0·80	0·963	0·195
0·30	1·102	0·257	0·85	0·876	0·179
0·35	1·113	0·254	0·90	0·751	0·160
0·40	1·122	0·251	0·95	0·557	0·138
0·45	1·127	0·248	1·00	0	0·113
0·50	1·128	0·244			

TABLE 24

Solution 20

Constant-chord wing, aspect ratio 4, 45 *deg sweep-back,* 126-*vortex* 6-*point standard solution modified: auxiliary solution*

a_0'	$0\cdot02504$	p_0	$-0\cdot30052$	$dc_L/d\alpha = 3\cdot039$
a_1'	$-0\cdot04137$	p_1	$0\cdot45074$	

η	C_{LL}/C_L	Local a.c.	η	C_{LL}/C_L	Local a.c.
0	0·964	0·344	0·50	1·132	0·246
0·05	0·984	0·328	0·60	1·119	0·235
0·10	1·018	0·302	0·70	1·072	0·218
0·15	1·045	0·284	0·80	0·966	0·195
0·20	1·068	0·270	0·90	0·752	0·164
0·30	1·101	0·257	0·95	0·557	0·146
0·40	1·123	0·253	1·00	0	0·125

TABLE 25

Solution 21

Rectangular wing, aspect ratio 2, 126-*vortex* 6-*point standard solution:* $\eta = 0\cdot2,\ 0\cdot6,\ 0\cdot8$

a_0	$0\cdot14153$	c_1	$-0\cdot02988$	$dc_L/d\alpha = 2\cdot524$
a_1	$-0\cdot03065$	e_0	$0\cdot00754$	$C_{DI} = 1\cdot001\,\frac{1}{\pi A}\,C_L^2$
c_0	$0\cdot02135$	e_1	$-0\cdot01406$	

Aerodynamic centre $0\cdot2110\bar{c}$ behind leading edge.

η	C_{LL}/C_L	Local a.c.	η	C_{LL}/C_L	Local a.c.
0	1·257	0·220	0·55	1·066	0·210
0·05	1·255	0·220	0·60	1·024	0·208
0·10	1·251	0·219	0·65	0·976	0·206
0·15	1·244	0·219	0·70	0·921	0·203
0·20	1·234	0·218	0·75	0·856	0·200
0·25	1·221	0·218	0·80	0·780	0·197
0·30	1·204	0·217	0·85	0·688	0·193
0·35	1·184	0·216	0·90	0·572	0·189
0·40	1·161	0·215	0·95	0·412	0·185
0·45	1·134	0·214	1·00	0	0·180
0·50	1·102	0·212			

TABLE 26

Solution 22

Constant-chord wing, aspect ratio 2, 30 *deg sweep-back,* 126-*vortex standard* 6-*point solution*

a_0	$0 \cdot 12334$	c_1	$-0 \cdot 15199$	$dc_L/d\alpha = 2 \cdot 480$	
a_1	$-0 \cdot 00471$	e_0	$-0 \cdot 02948$	$C_{DI} = 1 \cdot 003 \dfrac{1}{\pi A} C_L^2$	
c_0	$0 \cdot 10075$	e_1	$0 \cdot 03426$		

Aerodynamic centre $0 \cdot 462\bar{c}$ behind apex.

η	C_{LL}/C_L	Local a.c.	η	C_{LL}/C_L	Local a.c.
0	1·226	0·245	0·55	1·078	0·203
0·05	1·225	0·245	0·60	1·040	0·196
0·10	1·222	0·244	0·65	0·995	0·189
0·15	1·218	0·242	0·70	0·942	0·182
0·20	1·211	0·239	0·75	0·878	0·174
0·25	1·202	0·236	0·80	0·801	0·167
0·30	1·190	0·232	0·85	0·707	0·159
0·35	1·176	0·227	0·90	0·587	0·151
0·40	1·158	0·222	0·95	0·422	0·143
0·45	1·136	0·216	1·00	0	0·135
0·50	1·109	0·210			

TABLE 27

Solution 23

Constant-chord wing, aspect ratio 2, 30 *deg sweep-back,* 126-*vortex standard* 6-*point solution modified by auxiliary solution*

a_0'	$0 \cdot 01455$	p_0	$-0 \cdot 20014$	$dc_L/d\alpha = 2 \cdot 441$
a_1'	$-0 \cdot 02794$	p_1	$0 \cdot 34280$	$C_{DI} = 1 \cdot 005 \dfrac{1}{\pi A} C_L^2$

Aerodynamic centre $0 \cdot 469\bar{c}$ behind apex.

η	C_{LL}/C_L	Local a.c.	η	C_{LL}/C_L	Local a.c.
0	1·198	0·282	0·55	1·084	0·203
0·05	1·201	0·276	0·60	1·047	0·196
0·10	1·206	0·266	0·65	1·003	0·189
0·15	1·207	0·256	0·70	0·949	0·182
0·20	1·205	0·248	0·75	0·886	0·174
0·25	1·199	0·241	0·80	0·808	0·167
0·30	1·190	0·234	0·85	0·714	0·159
0·35	1·177	0·227	0·90	0·593	0·151
0·40	1·161	0·222	0·95	0·426	0·143
0·45	1·140	0·216	1·00	0	0·135
0·50	1·115	0·210			

TABLE 28

Solution 24

Constant-chord wing, aspect ratio 2, 45 *deg sweep-back,* 126-*vortex* 6-*point standard solution*

a_0	$0 \cdot 10315$	c_1	$-0 \cdot 18082$	$dc_L/d\alpha$	$= 2 \cdot 359$
a_1	$0 \cdot 01680$	e_0	$-0 \cdot 03370$	C_{DI}	$= 1 \cdot 009 \dfrac{1}{\pi A} C_L^2$
c_0	$0 \cdot 13559$	e_1	$0 \cdot 01396$		

Aerodynamic centre $0 \cdot 661 \bar{c}$ behind apex.

η	C_{LL}/C_L	Local a.c.	η	C_{LL}/C_L	Local a.c.
0	1·188	0·269	0·55	1·092	0·213
0·05	1·188	0·268	0·60	1·060	0·203
0·10	1·187	0·267	0·65	1·019	0·193
0·15	1·186	0·264	0·70	0·968	0·183
0·20	1·183	0·261	0·75	0·906	0·172
0·25	1·179	0·256	0·80	0·828	0·160
0·30	1·173	0·251	0·85	0·731	0·148
0·35	1·164	0·244	0·90	0·607	0·135
0·40	1·153	0·238	0·95	0·434	0·121
0·45	1·138	0·230	1·00	0	0·106
0·50	1·118	0·222			

TABLE 29

Solution 25

Constant-chord wing, aspect ratio 2, 45 *deg sweep-back,* 126-*vortex* 6-*point standard solution modified by auxiliary solution*

a_0'	$0 \cdot 02633$	p_0	$-0 \cdot 34507$	$dc_L/d\alpha$	$= 2 \cdot 300$
a_1'	$-0 \cdot 04655$	p_1	$0 \cdot 55418$	C_{DI}	$= 1 \cdot 019 \dfrac{1}{\pi A} C_L^2$

Aerodynamic centre $0 \cdot 676 \bar{c}$ behind apex.

η	C_{LL}/C_L	Local a.c.	η	C_{LL}/C_L	Local a.c.
0	1·117	0·337	0·55	1·108	0·213
0·05	1·128	0·326	0·60	1·077	0·203
0·10	1·145	0·306	0·65	1·038	0·193
0·15	1·159	0·290	0·70	0·987	0·183
0·20	1·168	0·276	0·75	0·925	0·172
0·25	1·172	0·264	0·80	0·846	0·160
0·30	1·172	0·254	0·85	0·748	0·148
0·35	1·168	0·244	0·90	0·621	0·135
0·40	1·161	0·238	0·95	0·445	0·121
0·45	1·149	0·230	1·00	0	0·106
0·50	1·132	0·222			

TABLE 30

Solution 26

Square wing, aspect ratio 1, 84-*vortex* 6-*point standard solution:* $\eta = 0 \cdot 2, 0 \cdot 6, 0 \cdot 8$

a_0	0·20900	c_1	− 0·01109	$dc_L/d\alpha = 1 \cdot 489$	
a_1	− 0·11680	e_0	0·00839	$C_{DI} = 1 \cdot 000 \dfrac{1}{\pi A} C_L^2$	
c_0	0·00640	e_1	− 0·01657		

Aerodynamic centre $0 \cdot 1482\bar{c}$ behind leading edge.

Loading

η	C_{LL}/C_L	Local a.c.	η	C_{LL}/C_L	Local a.c.
0	1·271	0·153	0·55	1·064	0·149
0·05	1·270	0·153	0·60	1·019	0·148
0·10	1·265	0·153	0·65	0·969	0·147
0·15	1·257	0·153	0·70	0·911	0·146
0·20	1·246	0·153	0·75	0·844	0·144
0·25	1·231	0·152	0·80	0·766	0·142
0·30	1·213	0·152	0·85	0·673	0·140
0·35	1·192	0·152	0·90	0·557	0·137
0·40	1·166	0·151	0·95	0·399	0·134
0·45	1·137	0·151	1·00	0	0·131
0·50	1·103	0·150			

Induced camber

Position on chord	Spanwise location: value of η			
	0	0·8	0·9	0·95
0	0	0	0	0
0·1	− 0·014	− 0·010	− 0·007	− 0·005
0·2	− 0·025	− 0·017	− 0·013	− 0·009
0·3	− 0·033	− 0·022	− 0·017	− 0·012
0·4	− 0·038	− 0·025	− 0·019	− 0·014
0·5	− 0·039	− 0·026	− 0·020	− 0·015
0·6	− 0·038	− 0·025	− 0·019	− 0·014
0·7	− 0·033	− 0·022	− 0·017	− 0·012
0·8	− 0·025	− 0·017	− 0·013	− 0·009
0·9	− 0·014	− 0·010	− 0·007	− 0·005
1·0	0	0	0	0

(22304) C

TABLE 31

Solution 27

Constant-chord wing, aspect ratio 1, 30 *deg sweep-back,* 126-*vortex* 6-*point standard solution:* $\eta = 0 \cdot 2,\ 0 \cdot 6,\ 0 \cdot 8$

a_0	$0 \cdot 19336$	c_1	$-\ 0 \cdot 13039$	$dc_L/d\alpha = 1 \cdot 493$	
a_1	$-\ 0 \cdot 08460$	e_0	$-\ 0 \cdot 02761$	$C_{DI} = 1 \cdot 000 \dfrac{1}{\pi A} C_L^2$	
c_0	$0 \cdot 06674$	e_1	$0 \cdot 05322$		

Aerodynamic centre $0 \cdot 281\bar{c}$ behind apex.

Loading

η	C_{LL}/C_L	Local a.c.	η	C_{LL}/C_L	Local a.c.
0	1·271	0·180	0·55	1·064	0·152
0·05	1·270	0·180	0·60	1·020	0·147
0·10	1·265	0·179	0·65	0·969	0·143
0·15	1·257	0·178	0·70	0·911	0·138
0·20	1·246	0·176	0·75	0·844	0·134
0·25	1·232	0·174	0·80	0·766	0·129
0·30	1·214	0·171	0·85	0·672	0·126
0·35	1·192	0·168	0·90	0·556	0·122
0·40	1·167	0·164	0·95	0·398	0·119
0·45	1·137	0·160	1·00	0	0·117
0·50	1·103	0·156			

Induced camber

Position on chord	Spanwise location: value of η			
	0	0·8	0·9	0·95
0	0	0	0	0
0·1	− 0·010	− 0·011	− 0·008	− 0·006
0·2	− 0·018	− 0·019	− 0·014	− 0·011
0·3	− 0·024	− 0·025	− 0·019	− 0·014
0·4	− 0·027	− 0·028	− 0·022	− 0·016
0·5	− 0·028	− 0·029	− 0·023	− 0·017
0·6	− 0·027	− 0·028	− 0·022	− 0·016
0·7	− 0·024	− 0·025	− 0·019	− 0·014
0·8	− 0·018	− 0·019	− 0·014	− 0·011
0·9	− 0·010	− 0·011	− 0·008	− 0·006
1·0	0	0	0	0

TABLE 32

Solution 28

Constant-chord wing, aspect ratio 1, 30 *deg sweep-back,* 126-*vortex* 6-*point standard solution modified by auxiliary solution*

a_0'	$0\cdot00519$	p_0	$-0\cdot10036$	$dc_L/d\alpha$	$= 1\cdot486$
a_1'	$-0\cdot01125$	p_1	$0\cdot19381$	C_{DI}	$= 1\cdot000 \frac{1}{\pi A} C_L^2$

Aerodynamic centre $0\cdot287\bar{c}$ behind apex.

Loading

η	C_{LL}/C_L	Local a.c.	η	C_{LL}/C_L	Local a.c.
0	1·268	0·201	0·55	1·065	0·153
0·05	1·267	0·199	0·60	1·020	0·148
0·10	1·263	0·194	0·65	0·970	0·143
0·15	1·256	0·189	0·70	0·912	0·138
0·20	1·245	0·185	0·75	0·844	0·134
0·25	1·231	0·180	0·80	0·766	0·129
0·30	1·214	0·176	0·85	0·673	0·126
0·35	1·192	0·172	0·90	0·557	0·122
0·40	1·167	0·168	0·95	0·399	0·119
0·45	1·138	0·163	1·00	0	0·117
0·50	1·104	0·158			

Induced camber

Position on chord	Spanwise location: value of η			
	0	0·8	0·9	0·95
0	0	0	0	0
0·1	− 0·007	− 0·011	− 0·008	− 0·006
0·2	− 0·013	− 0·019	− 0·015	− 0·011
0·3	− 0·016	− 0·025	− 0·019	− 0·014
0·4	− 0·019	− 0·028	− 0·022	− 0·016
0·5	− 0·020	− 0·030	− 0·023	− 0·017
0·6	− 0·019	− 0·028	− 0·022	− 0·016
0·7	− 0·016	− 0·025	− 0·019	− 0·014
0·8	− 0·013	− 0·019	− 0·015	− 0·011
0·9	− 0·007	− 0·011	− 0·008	− 0·006
1·0	0	0	0	0

TABLE 33

Solution 29

Constant-chord wing, aspect ratio 1, 45 *deg sweep-back,* 126-*vortex* 6-*point standard solution:* $\eta = 0{\cdot}2,\ 0{\cdot}6,\ 0{\cdot}8$

a_0	$0{\cdot}16730$	c_1	$-\ 0{\cdot}26228$	$dc_L/d\alpha$	$= 1{\cdot}484$
a_1	$-\ 0{\cdot}03574$	e_0	$-\ 0{\cdot}07894$	C_{DI}	$= 1{\cdot}000 \dfrac{1}{\pi A} C_L^2$
c_0	$0{\cdot}13721$	e_1	$0{\cdot}14867$		

Aerodynamic centre $0{\cdot}394\bar{c}$ behind apex.

Loading

η	C_{LL}/C_L	Local a.c.	η	C_{LL}/C_L	Local a.c.
0	1·265	0·220	0·55	1·067	0·166
0·05	1·264	0·220	0·60	1·023	0·158
0·10	1·259	0·218	0·65	0·973	0·151
0·15	1·252	0·215	0·70	0·915	0·144
0·20	1·242	0·212	0·75	0·848	0·138
0·25	1·228	0·207	0·80	0·769	0·132
0·30	1·211	0·202	0·85	0·675	0·128
0·35	1·190	0·195	0·90	0·558	0·126
0·40	1·166	0·189	0·95	0·400	0·125
0·45	1·138	0·181	1·00	0	0·126
0·50	1·105	0·174			

Induced camber

Position on chord	Spanwise location: value of η			
	0	0·8	0·9	0·95
0	0	0	0	0
0·1	− 0·004	− 0·010	− 0·008	− 0·006
0·2	− 0·008	− 0·018	− 0·014	− 0·010
0·3	− 0·010	− 0·024	− 0·019	− 0·013
0·4	− 0·012	− 0·028	− 0·021	− 0·015
0·5	− 0·012	− 0·029	− 0·022	− 0·016
0·6	− 0·012	− 0·028	− 0·021	− 0·015
0·7	− 0·010	− 0·024	− 0–019	− 0·013
0·8	− 0·008	− 0·018	− 0·014	− 0·010
0·9	− 0·004	− 0·010	− 0·008	− 0·006
1·0	0	0	0	0

TABLE 34

Solution 30

Constant-chord wing, aspect ratio 1, 45 *deg sweep-back,* 126-*vortex* 6-*point standard solution modified by auxiliary solution*

a_0'	$0\cdot01300$	p_{a1}	$0\cdot17130$	$dC_L/d\alpha = 1\cdot469$
a_1'	$-\ 0\cdot02620$	p_{b0}	$-\ 0\cdot11582$	$C_{DI} = 1\cdot000\ \dfrac{1}{\pi A}\ C_L^2$
p_{a0}	$-\ 0\cdot09363$	p_{b1}	$0\cdot21654$	

Aerodynamic centre $0\cdot405\bar{c}$ behind apex.

Loading

η	C_{LL}/C_L	Local a.c.	η	C_{LL}/C_L	Local a.c.
0	1·252	0·263	0·55	1·070	0·167
0·05	1·253	0·258	0·60	1·026	0·158
0·10	1·252	0·248	0·65	0·976	0·151
0·15	1·247	0·238	0·70	0·918	0·144
0·20	1·239	0·228	0·75	0·851	0·138
0·25	1·227	0·220	0·80	0·772	0·132
0·30	1·211	0·211	0·85	0·678	0·128
0·35	1·191	0·203	0·90	0·561	0·126
0·40	1·168	0·194	0·95	0·402	0·125
0·45	1·140	0·185	1·00	0	0·126
0·50	1·107	0·176			

Induced camber

Position on chord	Spanwise location: value of η			
	0	0·8	0·9	0·95
0	0	0	0	0
0·1	0·002	− 0·011	− 0·008	− 0·006
0·2	0·003	− 0·019	− 0·015	− 0·011
0·3	0·004	− 0·025	− 0·020	− 0·014
0·4	0·005	− 0·029	− 0·022	− 0·016
0·5	0·005	− 0·030	− 0·023	− 0·017
0·6	0·005	− 0·029	− 0·022	− 0·016
0·7	0·004	− 0·025	− 0·020	− 0·014
0·8	0·003	− 0·019	− 0·015	− 0·011
0·9	0·002	− 0·011	− 0·008	− 0·006
1·0	0	0	0	0

(22304) C*

TABLE 35

Solution 31

Triangular wing, 90 *deg apex angle, aspect ratio* 4, *standard* 126-*vortex* 6-*point solution:*
$\eta = 0{\cdot}2,\ 0{\cdot}6,\ 0{\cdot}8$

a_0	0·08851	c_1	− 0·04994	$dc_L/d\alpha = 3{\cdot}470$	
a_1	0·01339	e_0	− 0·02830	$C_{DI} = 1{\cdot}026 \dfrac{1}{\pi A} C_L^2$	
c_0	0·00187	e_1	0·03216		

Aerodynamic centre $1{\cdot}116\bar{c}$ behind apex.

η	C_{LL}/C_L	$C_{LL}c/C_L\bar{c}$	Local a.c.	η	C_{LL}/C_L	$C_{LL}c/C_L\bar{c}$	Local a.c.
0	0·690	1·379	0·268	0·55	1·171	1·054	0·252
0·05	0·724	1·376	0·267	0·60	1·236	0·989	0·249
0·10	0·760	1·369	0·267	0·65	1·309	0·916	0·247
0·15	0·798	1·356	0·266	0·70	1·396	0·837	0·245
0·20	0·836	1·338	0·265	0·75	1·501	0·751	0·243
0·25	0·876	1·314	0·264	0·80	1·639	0·655	0·241
0·30	0·918	1·285	0·262	0·85	1·835	0·550	0·240
0·35	0·962	1·251	0·268	0·90	2·162	0·432	0·239
0·40	1·009	1·211	0·258	0·95	2·913	0·291	0·239
0·45	1·059	1·165	0·256	1·00		0	0·241
0·50	1·112	1·112	0·254				

TABLE 36

Solution 32

Triangular wing, 90 *deg apex angle, aspect ratio* 4, *standard* 126-*vortex* 6-*point solution modified by* 4-*point conditional auxiliary solution*

a_0'	0·01304	p_0'	− 0·17388	$dc_L/d\alpha = 3{\cdot}470$
a_1'	− 0·02608	p_1'	0·34776	$C_{DI} = 1{\cdot}026 \dfrac{1}{\pi A} C_L^2$

Aerodynamic centre $1{\cdot}133\bar{c}$ behind apex.

η	C_{LL}/C_L	$C_{LL}c/C_L\bar{c}$	Local a.c.	η	C_{LL}/C_L	$C_{LL}c/C_L\bar{c}$	Local a.c.
0	0·690	1·379	0·314	0·55	1·171	1·054	0·252
0·05	0·724	1·376	0·308	0·60	1·236	0·989	0·249
0·10	0·760	1·369	0·296	0·65	1·309	0·916	0·247
0·15	0·798	1·356	0·286	0·70	1·396	0·837	0·245
0·20	0·836	1·338	0·278	0·75	1·501	0·751	0·243
0·25	0·876	1·314	0·272	0·80	1·639	0·655	0·241
0·30	0·918	1·285	0·267	0·85	1·835	0·550	0·240
0·35	0·962	1·251	0·262	0·90	2·162	0·432	0·239
0·40	1·009	1·211	0·258	0·95	2·913	0·291	0·239
0·45	1·059	1·165	0·256	1·00		0	0·241
0·50	1·112	1·112	0·254				

TABLE 37

Solution 33

Triangular wing, 90 *deg angle, with tips cropped to aspect ratio* 3, *standard* 126-*vortex* 6-*point solution*: $\eta = 0{\cdot}2,\ 0{\cdot}6,\ 0{\cdot}8$

a_0	$0{\cdot}10118$	c_1	$-0{\cdot}07024$	$dc_L/d\alpha$	$= 3{\cdot}142$
a_1	$0{\cdot}01426$	e_0	$-0{\cdot}00869$	C_{DI}	$= 1{\cdot}001 \dfrac{1}{\pi A} C_L^2$
c_0	$0{\cdot}02309$	e_1	$0{\cdot}03020$		

Aerodynamic centre $0{\cdot}916\bar{c}$ behind apex.

η	C_{LL}/C_L	$C_{LL}c/C_L\bar{c}$	Local a.c.	η	C_{LL}/C_L	$C_{LL}c/C_L\bar{c}$	Local a.c.
0	0·743	1·300	0·266	0·55	1·141	1·055	0·245
0·05	0·775	1·298	0·266	0·60	1·184	1·006	0·242
0·10	0·807	1·292	0·266	0·65	1·228	0·952	0·238
0·15	0·841	1·282	0·265	0·70	1·273	0·891	0·234
0·20	0·874	1·268	0·263	0·75	1·316	0·822	0·231
0·25	0·909	1·250	0·262	0·80	1·352	0·743	0·228
0·30	0·945	1·228	0·260	0·85	1·371	0·651	0·225
0·35	0·981	1·202	0·257	0·90	1·344	0·538	0·222
0·40	1·019	1·172	0·254	0·95	1·184	0·385	0·220
0·45	1·058	1·137	0·252	1·00	0	0	0·219
0·50	1·099	1·099	0·248				

TABLE 38

Solution 34

Triangular wing, 90 *deg apex angle, with tips cropped to aspect ratio* 3, 8-*point solution*: $\eta = 0,\ 0{\cdot}2,\ 0{\cdot}6,\ 0{\cdot}8$

a_0	$0{\cdot}11415$	e_0	$0{\cdot}00028$	$dc_L/d\alpha$	$= 3{\cdot}123$
a_1	$-0{\cdot}01434$	e_1	$0{\cdot}00967$	C_{DI}	$= 1{\cdot}001 \dfrac{1}{\pi A} C_L^2$
c_0	$0{\cdot}00975$	p_0	$-0{\cdot}17274$		
c_1	$-0{\cdot}03973$	p_1	$0{\cdot}35454$		

Aerodynamic centre $0{\cdot}929\bar{c}$ behind apex.

η	C_{LL}/C_L	$C_{LL}c/C_L\bar{c}$	Local a.c.	η	C_{LL}/C_L	$C_{LL}c/C_L\bar{c}$	Local a.c.
0	0·744	1·301	0·306	0·55	1·141	1·055	0·246
0·05	0·775	1·298	0·300	0·60	1·185	1·007	0·242
0·10	0·807	1·291	0·290	0·65	1·230	0·953	0·239
0·15	0·840	1·280	0·281	0·70	1·275	0·892	0·235
0·20	0·873	1·266	0·274	0·75	1·318	0·824	0·232
0·25	0·908	1·248	0·269	0·80	1·354	0·745	0·228
0·30	0·943	1·226	0·265	0·85	1·373	0·652	0·224
0·35	0·980	1·201	0·261	0·90	1·347	0·539	0·221
0·40	1·018	1·171	0·257	0·95	1·186	0·385	0·218
0·45	1·058	1·137	0·253	1·00	0	0	0·214
0·50	1·098	1·098	0·250				

TABLE 39

Solution 35

Triangular wing, 90 *deg apex angle, with tips cropped to aspect ratio* 2·309, *standard* 126-*vortex* 6-*point solution*

a_0	0·11541	c_1	$-$ 0·08365	$dc_L/d\alpha = 2{\cdot}761$	
a_1	0·01165	e_0	0·01183	$C_{DI} = 1{\cdot}000 \dfrac{1}{\pi A} C_L^2$	
c_0	0·03985	e_1	$-$ 0·01769	$\lambda =$ [illegible]	

Aerodynamic centre $0{\cdot}756\bar{c}$ behind apex.

η	C_{LL}/C_L	$C_{LL}c/C_L\bar{c}$	Local a.c.	η	C_{LL}/C_L	$C_{LL}c/C_L\bar{c}$	Local a.c.
0	0·808	1·274	0·262	0·55	1·127	1·062	0·234
0·05	0·838	1·273	0·262	0·60	1·150	1·017	0·228
0·10	0·867	1·268	0·261	0·65	1·168	0·966	0·222
0·15	0·897	1·260	0·260	0·70	1·181	0·908	0·215
0·20	0·927	1·248	0·258	0·75	1·184	0·842	0·208
0·25	0·957	1·233	0·256	0·80	1·170	0·764	0·199
0·30	0·986	1·214	0·254	0·85	1·128	0·672	0·190
0·35	1·016	1·192	0·251	0·90	1·036	0·557	0·180
0·40	1·045	1·166	0·248	0·95	0·833	0·400	0·170
0·45	1·074	1·136	0·244	1·00	0	0	0·158
0·50	1·101	1·101	0·239				

TABLE 40

Solution 36

Triangular wing, 90 *deg apex angle, with tips cropped to aspect ratio* 2·309, *standard* 126-*vortex* 6-*point solution modified by conditional* 4-*point auxiliary solution*

a_0'	0·00882	p_0	$-$ 0·14653	$dc_L/d\alpha = 2{\cdot}761$
a_1'	$-$ 0·01764	p_1	0·29306	$C_{DI} = 1{\cdot}000 \dfrac{1}{\pi A} C_L^2$

Aerodynamic centre $0{\cdot}767\bar{c}$ behind apex.

η	C_{LL}/C_L	$C_{LL}c/C_L\bar{c}$	Local a.c.	η	C_{LL}/C_L	$C_{LL}c/C_L\bar{c}$	Local a.c.
0	0·808	1·274	0·298	0·55	1·127	1·062	0·235
0·05	0·838	1·273	0·293	0·60	1·150	1·017	0·228
0·10	0·867	1·268	0·284	0·65	1·168	0·966	0·222
0·15	0·897	1·260	0·278	0·70	1·181	0·908	0·215
0·20	0·927	1·248	0·272	0·75	1·184	0·842	0·208
0·25	0·957	1·233	0·266	0·80	1·170	0·764	0·199
0·30	0·986	1·214	0·262	0·85	1·128	0·672	0·190
0·35	1·016	1·192	0·257	0·90	1·036	0·557	0·180
0·40	1·045	1·166	0·252	0·95	0·833	0·400	0·170
0·45	1·074	1·136	0·247	1·00	0	0	0·158
0·50	1·101	1·101	0·241				

TABLE 41

Experimental and theoretical lift and aerodynamic centre for a delta wing, apex angle 90 deg with pointed and cropped tips

Aspect ratio	$dc_L/d\alpha$		Ratio
	Wind tunnel	Theoretical	
4	3·342	3·547	0·942
3	3·048	3·192	0·955
2·31	2·720	2·821	0·964

Aspect ratio	a.c. in terms of $\bar{c}$ behind apex		Difference
	Wind tunnel	Theoretical	
4	1·126	1·133	− 0·007
3	0·943	0·929	0·014
2·31	0·784	0·767	0·017

Note:—The theoretical values of $dc_L/d\alpha$ have been multiplied by the correction factor 1·022.

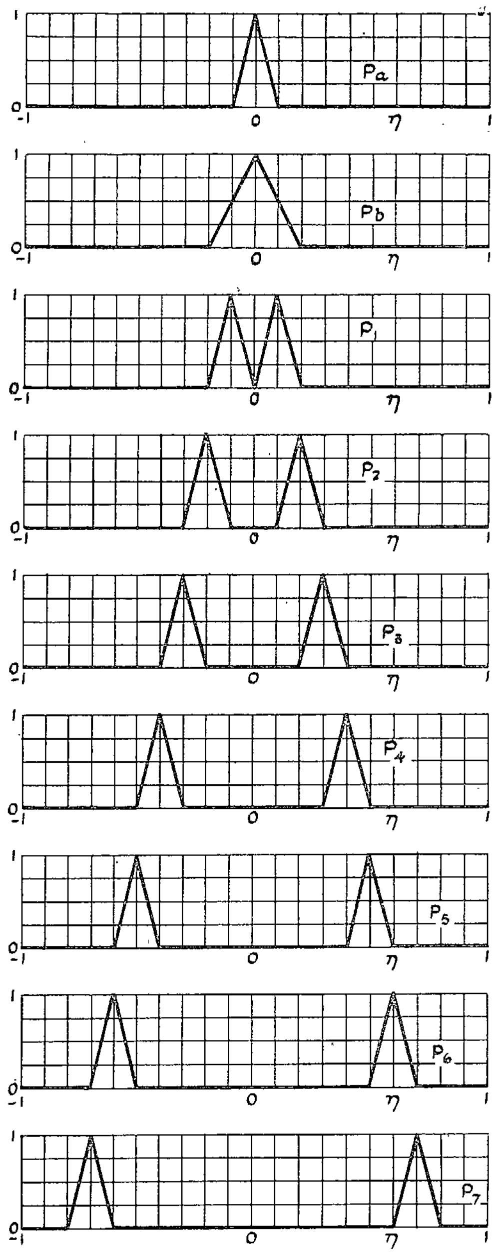

FIG. 1. Spanwise distribution of induced downwash for P functions.

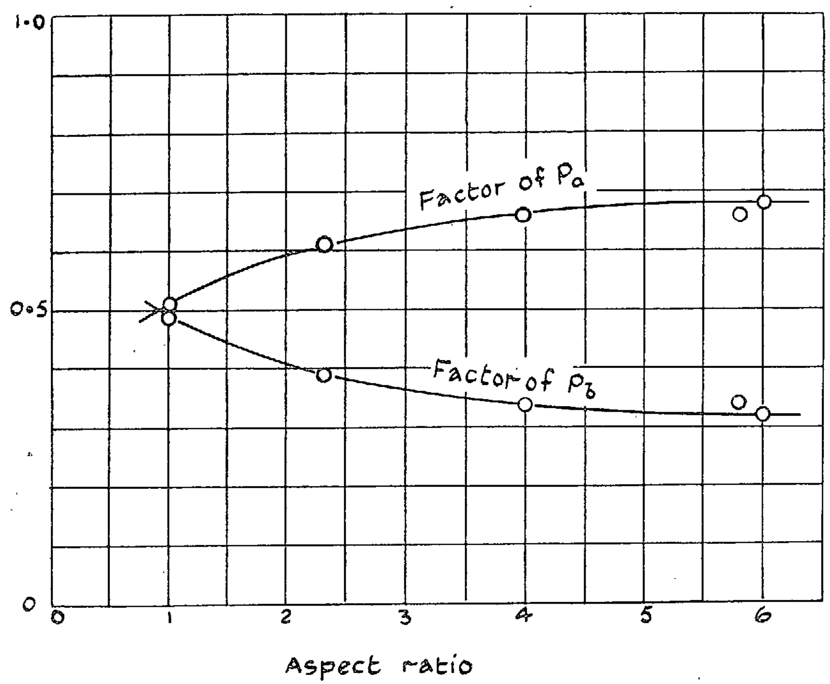

FIG. 2. Proportions of P_a and P_b for combined circulation function to allow for discontinuity at median section.

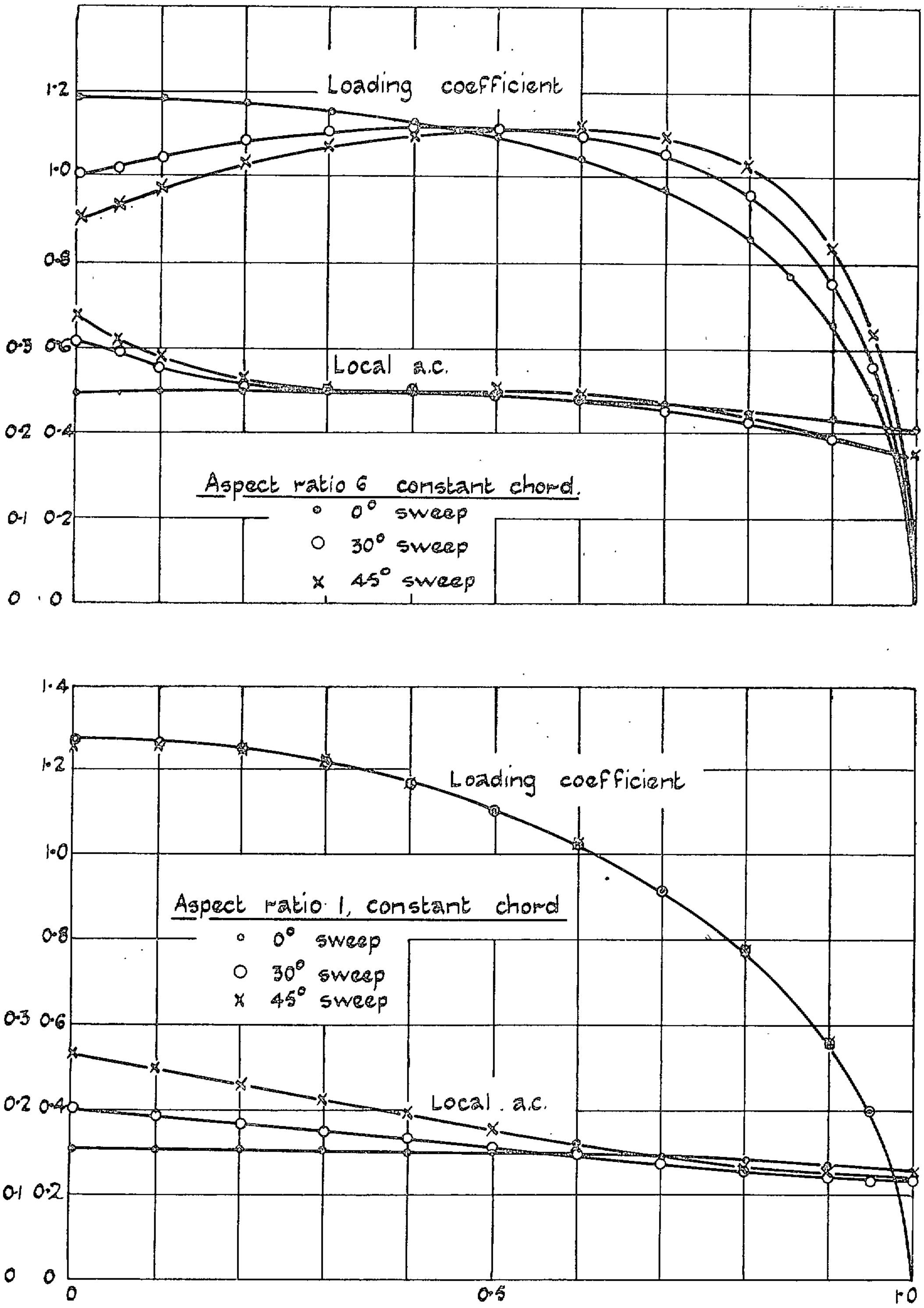

FIG. 3. Loading coefficient and local aerodynamic centre for two wings of constant chord.

(22304) Wt. 15-680 K9 4/52 F. M. & S.

PRINTED IN GREAT BRITAIN

R. & M. No. 2596
(11,542)
A.R.C. Technical Report

Publications of the Aeronautical Research Council

ANNUAL TECHNICAL REPORTS OF THE AERONAUTICAL RESEARCH COUNCIL (BOUND VOLUMES)—

1934–35 Vol. I. Aerodynamics. *Out of print.*
Vol. II. Seaplanes, Structures, Engines, Materials, etc. 40*s.* (40*s.* 8*d.*)

1935–36 Vol. I. Aerodynamics. 30*s.* (30*s.* 7*d.*)
Vol. II. Structures, Flutter, Engines, Seaplanes, etc. 30*s.* (30*s.* 7*d.*)

1936 Vol. I. Aerodynamics General, Performance, Airscrews, Flutter and Spinning. 40*s.* (40*s.* 9*d.*)
Vol. II. Stability and Control, Structures, Seaplanes, Engines, etc. 50*s.* (50*s.* 10*d.*)

1937 Vol. I. Aerodynamics General, Performance, Airscrews, Flutter and Spinning. 40*s.* (40*s.* 10*d.*)
Vol. II. Stability and Control, Structures, Seaplanes, Engines, etc. 60*s.* (61*s.*)

1938 Vol. I. Aerodynamics General, Performance, Airscrews. 50*s.* (51*s.*)
Vol. II. Stability and Control, Flutter, Structures, Seaplanes, Wind Tunnels, Materials. 30*s.* (30*s.* 9*d.*)

1939 Vol. I. Aerodynamics General, Performance, Airscrews, Engines. 50*s.* (50*s.* 11*d.*)
Vol. II. Stability and Control, Flutter and Vibration, Instruments, Structures, Seaplanes, etc. 63*s.* (64*s.* 2*d.*)

1940 Aero and Hydrodynamics, Aerofoils, Airscrews, Engines, Flutter, Icing, Stability and Control, Structures, and a miscellaneous section. 50*s.* (51*s.*)

Certain other reports proper to the 1940 volume will subsequently be included in a separate volume.

ANNUAL REPORTS OF THE AERONAUTICAL RESEARCH COUNCIL—

1933–34	1*s.* 6*d.* (1*s.* 8*d.*)
1934–35	1*s.* 6*d.* (1*s.* 8*d.*)
April 1, 1935 to December 31, 1936.	4*s.* (4*s.* 4*d.*)
1937	2*s.* (2*s.* 2*d.*)
1938	1*s.* 6*d.* (1*s.* 8*d.*)
1939–48	3*s.* (3*s.* 2*d.*)

INDEX TO ALL REPORTS AND MEMORANDA PUBLISHED IN THE ANNUAL TECHNICAL REPORTS, AND SEPARATELY—

April, 1950 R. & M. No. 2600. 2*s.* 6*d.* (2*s.* 7½*d.*)

INDEXES TO THE TECHNICAL REPORTS OF THE AERONAUTICAL RESEARCH COUNCIL—

December 1, 1936 — June 30, 1939.	R. & M. No. 1850.	1*s.* 3*d.* (1*s.* 4½*d.*)
July 1, 1939 — June 30, 1945.	R. & M. No. 1950.	1*s.* (1*s.* 1½*d.*)
July 1, 1945 — June 30, 1946.	R. & M. No. 2050.	1*s.* (1*s.* 1½*d.*)
July 1, 1946 — December 31, 1946.	R. & M. No. 2150.	1*s.* 3*d.* (1*s.* 4½*d.*)
January 1, 1947 — June 30, 1947.	R. & M. No. 2250.	1*s.* 3*d.* (1*s.* 4½*d.*)

Prices in brackets include postage.

Obtainable from
HER MAJESTY'S STATIONERY OFFICE
York House, Kingsway, LONDON, W.C.2   423 Oxford Street, LONDON, W.1
P.O. Box 569, LONDON, S.E.1
13a Castle Street, EDINBURGH, 2   1 St. Andrew's Crescent, CARDIFF
39 King Street, MANCHESTER, 2   Tower Lane, BRISTOL, 1
2 Edmund Street, BIRMINGHAM, 3   80 Chichester Street, BELFAST
or through any bookseller.

S.O. Code No. 23-2596